

# **In vitro evaluation of wear properties of six orthodontic thermoplastic retainer materials**

Hani Ahdab DDS

A thesis submitted in partial fulfillment  
of the requirements for the degree  
of Master of Science in Orthodontics

Oregon Health and Sciences University  
Portland, OR

December 2016



## **Acknowledgements**

Thank you to my principal advisor Dr. Jack Ferracane for his advice throughout all stages of this project.

Thank you to my thesis committee members: Dr. Dan Yailen, Dr. David Covell, and Dr. Larry Doyle for their feedback and support of the project.

Thank you to Anna Hildebran for her help with sample fabrication.

Thank you Fuding Lin, Ph.D. and Camcor for their help with profilometer scanning of the samples

Thank you to my family: Judith, Emri, and Zowie for their love and support.

# Table of Contents

List of Figures .....	5
List of Tables .....	6
<b>Manuscript:</b>	
Title Page .....	7
Declaration of Interests .....	8
Abstract .....	9
Introduction .....	11
Materials and Methods .....	14
Results .....	17
Discussion .....	19
Conclusions .....	25
References .....	26
Figures Legends.....	31
Figures .....	35
Table Legends .....	50
Tables .....	51
<b>Literature Review:</b>	
Retention .....	53
Retainer History and VFR Fabrication .....	54
Attributes of VFR .....	55
Previous Research on VFR Materials .....	56
Wear Testing .....	57
Previous Research on VFR Wear .....	59
References .....	61
<b>Appendix A:</b> Recommendation and Future Research .....	66
<b>Appendix B:</b> Reported Values and Statistical Analysis .....	67
<b>Appendix C:</b> Images of Sample Fabrication .....	69

## List of Figures

Profilometer Imaging of Ace .....	35
Profilometer Imaging of Plus .....	36
Profilometer Imaging of Ultra.....	37
Profilometer Imaging of Endure .....	38
Profilometer Imaging of C+.....	39
Profilometer Imaging of Ultra.....	40
Barber-Colman Conversion Curves for GYZ-934-1 Impressor .....	41
Graph of Average Maximum Depth Loss.....	42
Graph of Average Net Weight Loss.....	43
Correlation of Average Weight Loss with Average Maximum Depth Loss.....	44
Graph of Average Volume Loss.....	45
Correlation of Vickers Hardness with Average Maximum Depth Loss.....	46
SEM Image of Unworn Surfaces of Samples at 500x Magnification.....	47
SEM Image of Worn Surfaces of Samples at 500x Magnification.....	48
SEM Image of Worn Surfaces of Samples at 1750x Magnification.....	49

## **List of Tables**

Table of Material Composition, Heating Time, Biostar Code, and Manufacturer.....	51
Table of Densities and Vickers Hardness Values for Each Group. ....	52

# **In vitro evaluation of wear properties of six orthodontic thermoplastic retainer materials**

Hani Ahdab DDS<sub>a</sub>

Daniel Yaillen DDS MSD<sub>a</sub>

Larry M. Doyle DDS<sub>a</sub>

David A. Covell Jr PhD DDS<sub>a</sub>

Jack L. Ferracane PhD<sub>b</sub>

a Department of Orthodontics, Oregon Health & Science University, Portland, OR

b Department of Restorative Dentistry, Oregon Health & Science University, Portland, OR

Corresponding Author:

Hani Ahdab DDS

E-mail: [ahdab.ortho@gmail.com](mailto:ahdab.ortho@gmail.com)

Phone: (949) 280-9609

## **Declaration of Interest**

None of the authors have any interest, financial or otherwise, in any of the thermoplastic materials involved in this study.



## **Abstract:**

**Introduction:** The use of vacuformed retainers (VFRs) for orthodontic retention is relatively common practice and evaluation of the physical properties of these thermoplastic materials is necessary to determine their longevity. VFRs have exhibited significant wear with long term use with differences observed between the various thermoplastic materials. Previous studies have examined the wear properties of these materials and determined that polyethylene copolymers have superior wear resistance than polypropylene copolymers. The aim of this study was to evaluate the in vitro wear resistance of various thermoplastic materials including polypropylene copolymers (PPC), polyethylene copolymers (PEC) and polyvinyl chloride polymers (PVC). **Materials and Methods:** Six thermoplastic materials were analyzed: two PPCs (Essix C+ and Invisacryl C), three PECs (Essix Plus, Essix ACE, Invisacryl Ultra) and one PVC (Endure). Net weight and volume loss, and maximum depth were analyzed to determine wear properties of the materials. The density and hardness of each material was also measured. The OHSU wear simulator was used to simulate in vitro two-body wear testing of the materials in water using 6.5 mm diameter steatite abrasers under a force of 45 N for 2,500 cycles. Samples were scanned with an optical laser profilometer and maximum depth was analyzed with Zygo software. Samples were weighed prior to and after wear testing to determine net weight loss. Densities of the materials were measured and used to calculate volume. Hardness was measured using a Barcol-type impressor. Wear surfaces were imaged with scanning electron microscope. **Results:** Endure showed significantly higher weight loss than C+ and Invisacryl C. Endure also showed greater wear depth than all other materials, and Ultra showed more wear depth than C+ and Invisacryl C. No statistical difference between groups was observed for

volume loss. Hardness correlated with wear depth by a second order polynomial relationship ( $R^2 = 0.94$ ). Weight loss was linearly correlated with volume loss ( $R^2 = 0.87$ ). Scanning electron microscopy showed greater tearing and scratching in PVC, followed by PEC, then PPC.

**Conclusions:** PVC displayed inferior wear resistance as compared with both PECs and PPCs based on both wear depth and weight loss. PECs performed similarly to PPCs with the exception of Ultra which had larger wear depths than both PPCs.

## Introduction:

Retention is the phase of orthodontic treatment aimed at maintaining the corrected dental arch and tooth positions after the completion of treatment<sup>1</sup>. Without proper retention, orthodontic relapse will occur and tooth position or arch relationship will have a tendency to return to their initial presentations prior to treatment<sup>1,2</sup>. Four factors have been implicated in causing orthodontic relapse: forces from periodontal and gingival tissues, forces from orofacial soft tissues, occlusal forces, and post treatment growth and development<sup>3</sup>. Gingival fibers require time to reorganize and remodel, taking approximately 4-6 months for the reorganization of the gingival collagen fibers and up to 232 days for elastic supracrestal fibers<sup>3,4</sup>. If the teeth are moved into an unstable position, forces from orofacial soft tissues or occlusal forces will cause relapse<sup>4</sup>. Unfavorable growth patterns associated with the development of malocclusion will continue through adult years and may contribute to a deterioration of occlusal relationships<sup>4,5</sup>. Even with completion of growth, relapse in the form of crowding has been shown to occur up to 20 years post-retention<sup>5</sup>.

There are various retainer types and designs as well as retention protocols used to maintain teeth and arches in the finished positions. In 1971 Ponitz<sup>6</sup> described the technique for fabrication of clear thermoplastic vacuum formed retainers (VFRs). The most common thermoplastic materials used to fabricate VFRs are polyethylene copolymers (PEC) and polypropylene polymers (PPC). Differences between the two polymers include that acrylic can be bonded to PEC and PEC is more esthetic due to the transparency of the material, whereas PPC is more durable and flexible<sup>7</sup>.

Benefits of using VFR's include ease of fabrication (requiring minimal time, skill and materials for construction) ease of delivery, and low cost<sup>8-10</sup>. The absence of any technical proficiency in wire bending allows delegation of the fabrication of VFRs to auxiliary personnel in the orthodontic office<sup>11</sup>. VFRs are also easily cleansable, small in size, and esthetic<sup>12</sup>. VFR survival times have been found in one study to be comparable with traditional Hawley retainers<sup>13</sup>. VFRs have been shown to hold corrections of lower anterior teeth more effectively than Hawley retainers and are more cost-effective<sup>14</sup>. The majority of patients also prefer VFRs to Hawley retainers, wearing them more leading to a higher satisfaction rate with their treatment<sup>15,16</sup>. Aside from retention, VFRs can also be used to produce minor tooth movements<sup>6,7</sup> or as bleaching trays<sup>17</sup>.

The major drawbacks of VFRs are their tendency to open the bite and their low durability<sup>9</sup>. VFRs have also been shown to inhibit relative vertical tooth eruption, or "settling" of the occlusion<sup>18</sup>. Low durability can result in broken VFRs, requiring additional financial cost to replace them, in addition to an increase in the risk of orthodontic relapse if the broken retainer is not replaced in a timely fashion. Common observations of orthodontists indicate that retainer fracture<sup>19</sup>, wear, and staining are problematic in orthodontic practice; however, there have been no reports of fracture frequency, or noncompliance as a result of staining or wear.

Wear is an important property used to assess the longevity of dental materials. The wear resistance of VFR thermoplastics has been investigated in two previous studies. Both studies<sup>7,11</sup> used steatite ceramic abrasers and measured wear depth to assess wear resistance. Gardner et al.<sup>11</sup> created wear on three different thermoplastics: Essix C+ (PPC), Invisacryl C (PPC) and TR (PEC), at a load of 25 kg (~245 N) for 1000 cycles in water at 37 °C.

After measuring the wear facets with laser profilometry, they concluded that the polyethylene co-polymer thermoplastic exhibited greater resistance to wear than the two polypropylene based thermoplastics. Raja et al.<sup>7</sup> studied four different thermoplastics: Essix C+ (PPC), Essix Ace (PEC), Duran (PEC), and Tru-Tain (PEC). The materials were subjected to 460 g of force (~4.5 N) at 1000 cycles. Wear changes assessed with mechanical surface profilometry showed that the three polyethylene co-polymers exhibited greater resistance to wear than the polypropylene based thermoplastic. Raja et al.<sup>7</sup> also found that Essix Ace had greater wear resistance than Tru-Tain. These two previous wear resistance studies show similar results indicating that under in vitro conditions, polyethylene co-polymers have superior wear resistance to polypropylene based thermoplastics<sup>7,11</sup>. However, no studies currently exist comparing these materials to polyvinyl chloride, another currently available option.

The objective of this study was to measure the wear resistance of six different thermoplastic materials: three polyethylene copolymers (PEC), two polypropylene copolymers (PPC), and one polyvinyl chloride polymer (PVC). Steatite abrasers were used for ease of standardization and to attempt to match the methodologies of previous studies<sup>11</sup>. Maximum wear depth, weight loss, and volume loss were evaluated to determine the wear characteristics of each thermoplastic material, and to correlate with their surface hardness. The hypothesis tested was that the PEC materials would be the most wear resistant of the three types of materials.

## **Materials and Methods:**

### **SAMPLE FABRICATION:**

Six thermoplastic materials were obtained from Raintree Essix and Great Lakes Orthodontics. Three of the materials were polyethylene copolymers (Essix Ace, Essix Plus, and Invisacryl Ultra), two were polypropylene polymers (Essix C+ and Invisacryl C), and one was a polyvinyl chloride polymer (Endure) (Table 1). The thermoplastic sheets, circular discs 1 mm in thickness and 125 mm in diameter, were formed over smoothed and soaped orthodontic stone slabs using a positive pressure machine (Biostar VI; ScheuBDental, Iserlohn, Germany) set to the manufacturer's recommended heating time (Table 1). Discs (n-12) were cut with a scissors from the formed surfaces of the thermoplastic materials and mounted in acrylic cylinders (25 mm diameter x 12 mm height) using epoxy resin. The surface of each sample was cleaned by swabbing with ethanol and visually inspected to ensure that there were no surface scratches or deformities.

### **FABRICATION OF STEATITE WEAR ABRADERS**

Steatite ceramic spheres (Fox Industries; Fairfield, NJ) with a diameter of 6.5 mm were cut in half using a slow speed diamond saw (Buehler Isomet Low Speed Saw; Illinois Tool Works) and used as the wear antagonists. The steatite hemispheres were mounted on nylon screws (supertough Nylon slot screw 1032 x 1 flat) using flowable light cured composite (Flow Tain; Reliance Orthodontics, Inc. Itasca, IL). The steatite antagonists were only used once and replaced with a fresh antagonist for each new specimen.

## WEAR TESTING

The samples were weighed prior to mounting in the wear machine. The wear testing was conducted on three OHSU oral wear simulators described in detail in a previous study<sup>20</sup>. The basic wear mechanism created by this machine is that an antagonist, attached to a piston mounted to a solenoid, is brought into contact with a sample under a constant, specified force and slid across the surface in water producing a wear trace of typically 4-6 mm in length. The antagonist is then lifted from the surface and returned to its original position for the next trace. Each wear machine is composed of two individual wear chambers. The specimens were placed in the individual wear chambers (six in total) and 3 ml of deionized water was added to simulate a two body wear test. Each of the materials being tested was rotated through the six different chambers to randomize any difference between the individual chambers and wear machines. The machines were set to transmit an abrasion force of  $45 \pm 1.3$  N for 2,500 cycles at 2 Hz. Prior to initiating the study, the machines were calibrated by measuring their force application during the sliding motion using a load cell mounted in a universal testing machine. Adjustments in the voltage applied to the solenoids were made to ensure that a uniform force, within a reasonable range of 43- 47 N, was delivered in each chamber/machine. Pilot testing was conducted on specimens of each material type in order to define the appropriate number of wear cycles to use in the experiment. This determination was made by ensuring that there was a difference in wear between the materials, but that no material wore through the full thickness of the sample. Because no sample wore through when the experiment was kept below 5-10,000 cycles, 2,500 cycles was chosen for the study.

After completion of the wear test, the samples were removed, cleaned with deionized water, and dried with compressed air. Subsequently, the samples were desiccated under vacuum pressure with Indicating Drierite (W.A Hammond Drierite Co, LTD; Xenia, OH) for 24 hrs to remove any fluids absorbed during the testing and reweighed. Weights of the samples prior to testing and after testing and subsequent desiccation were used to obtain a net weight loss due to material wear. The samples were then scanned with a laser profilometer (Zygo NewView 7300 optical 3D profilometer; CAMCOR, Eugene, OR) to image the wear facets, using the unworn adjacent areas as the original unworn surfaces. Zygo software was used to stitch together the scan and create a measurable surface map of each of the wear facets. Maximum wear depth was calculated as the difference in height between a point at the deepest portion of the wear facet and a point at the average of the adjacent edges of the unworn material adjacent to the wear facet (Figs. 1-6).

#### **MATERIAL PROPERTIES:**

The hardness of each of the thermoplastic materials was tested using a portable, hand-operated hardness tester (Barber–Colman Impressor, model GYZJ- 934; Rockford, Illinois). Three areas were analyzed on a vacuformed sheet of each material. The values were averaged and a conversion curve (Fig. 7) was used to estimate Vickers hardness.

The density of each type of thermoplastic material was also calculated using Archimedes method. Samples were weighed in air, then submerged in water and reweighed. Density was calculated as  $\rho = X \text{ (mass of specimen in air)} \div Y \text{ (mass of specimen in air – mass of specimen in water)} \times 0.99777$ , the latter being the density of water at 22°C. The density was calculated for two specimens for each material and was averaged. Using the density and weight loss of each



sample, the volume of material lost from the wear test was calculated as  $V \text{ (cm}^3\text{)} = \text{wt loss (g)} \div \text{density (g/cm}^3\text{)}$ .

## **SEM IMAGING**

One worn sample from Endure (PVC), C+ (PPC) and Ultra (PEC) was imaged with the scanning electron microscope (SEM). The samples were attached to the stub with carbon tape then painted with colloidal silver liquid (Tep Pella, INC, #1613, Tustin, CA) on the edges, avoiding the wear facet and surrounding area, to electrically ground the sample. The samples were sputter coated with an approximately 10 nm layer of gold palladium (Desk II Denton Vacuum, Moorestown, NJ) and imaged using the Quanta 200 SEM (FEI, Hillsboro, OR). SEM images were captured for unworn surfaces at 500x, worn surfaces in the center of the wear facet at 500x, and worn surfaces at 1750x of all three specimens.

## **STATISTICS:**

A one way ANOVA with a Post-hoc Tukey multiple comparison analysis was used to determine any variations between the groups when analyzing maximum wear depth, net weight loss, and net volume loss after the wear simulation ( $\alpha=0.05$ ). The null hypothesis to be tested was that there would be no difference in wear resistance among the materials. Scatter plots with  $R^2$  values of trend lines were used to determine any correlations between hardness and maximum wear depth, as well as weight loss with maximum wear depth.

## **Results:**

### **MAXIMUM DEPTH**

Differences were found among the mean wear depths of the groups, with Endure (PVC) demonstrating significantly greater wear depth than all of the other groups ( $p<0.01$ ), and Ultra

(PEC) having larger wear depth than C+ and Invisacrly C (PPC), with  $p < 0.01$  and  $p < 0.05$ , respectively (Fig. 8).

## **WEIGHT LOSS**

Average weight loss for each group due to wear (Fig. 9), demonstrated significant differences among the means of the groups ( $p = 0.016$ ). Endure, the only PVC polymer tested, showed a significantly greater weight loss (0.0066 g) than both PPCs, C+ and Invisacrly C (0.0050 g and 0.0049 g, respectively;  $p < 0.05$ ). No other differences were found.

## **WEIGHT LOSS VERSUS WEAR DEPTH**

A linear correlation ( $y = 9e^{-06}x + 0.0038$ ;  $R^2 = 0.8747$ ; Fig. 10) was observed between the wear depth and weight loss. Endure (PVC) demonstrated the largest weight loss and wear depth, while C+ (PPC) had the least amount of weight loss and wear depth.

## **VOLUMETRIC LOSS**

The densities (Table 2) and net weight loss were used to calculate the total volume of material lost according to the relationship  $V(\text{cm}^3) = \text{mass}(\text{g}) / \text{density}(\text{g}/\text{cm}^3)$ . The average volumetric loss for each sample was not statistically different among any of the groups (Fig. 11).

## **HARDNESS**

Average Vickers hardness values for each material were not equivalent (Table 2). The correlation between material hardness and maximum wear depth (Fig. 12) showed a direct relationship, with harder materials exhibiting greater wear depth. The values fit onto a second order polynomial with  $y = -0.0025x^2 + 1.3188x - 98.767$ ;  $R^2 = 0.9379$ . Endure (PVC) was the hardest material with a Vickers value of 70 and greatest wear depth. C+ (PPC) was the softest material with Vickers value of 25 and least wear depth.

## SEM IMAGES

SEM images of the unworn surface of the samples at 500x magnification (Fig. 13 A-C) show Ultra (PEC) to have the smoothest surface followed by C+ (PPC) then Endure (PVC). The worn surfaces at 500x magnification (Fig. 14 A-C) showed significant tearing and scratching of Endure (PVC), followed by Ultra (PEC), with the least amount in C+ (PPC). The surface tearing and lifting away was best seen at the 1750x magnification (Fig. 15 A-C).

## Discussion:

The results of this study demonstrate a difference in wear resistance between orthodontic thermoplastic materials with a clustering by material type. In terms of wear depth, Endure (PVC) had greater loss of material than all other samples, with Ultra (PEC) having greater loss than the materials in the PPC group. This result is contrary to that of Gardner et al.<sup>11</sup> and Raja et al.<sup>7</sup>, both of whom stated that PECs are about 3.7 times more wear resistant than PPCs based on measurements of wear depth. Other than the Ultra group, the other PECs (Ace and Plus) were not significantly different from the PPCs (C+ and Invisacryl C) in terms of wear resistance based on wear depth. The reason for the different outcomes in the studies is not obvious, although it is known that wear testing is highly variable and very dependent upon the mechanism of the specific testing machine.

Endure (PVC) had greater weight loss than the PPC groups, but was not significantly different from the PEC groups. There was no significant difference between the PEC and PPC groups. Weight loss has not been used in previous research to determine wear properties of thermoplastic materials used for orthodontic retention, likely due to difficulties in drying and

handling and their effect on the overall accuracy of the method. To determine whether the data is representative of actual wear of the samples a correlation analysis was conducted between weight loss and depth loss. A linear correlation with an  $R^2 = 0.87$  was observed (Fig. 10), with Endure (PVC) exhibiting the greatest depth and weight loss. The PPC groups are clustered together and show the least amount of weight and depth loss; they are followed by the cluster of PEC groups. This data suggests that weight loss was a fairly accurate surrogate measure for wear in this experiment. It is true that the accuracy of the weighing method is to some extent dependent upon having enough weight loss to be detectable, and this was not an issue in the current study.

After measuring the densities of the different materials, volume loss of each of the samples was obtained using the relationship between density and weight loss. Statistical analysis revealed no significant differences between any of the groups. Essentially the samples seem to have lost on average the same amount of volume during the wear test. This is an interesting observation because some of the groups like Endure (PVC) had greater depth loss than the other samples. This could be resultant from different lengths and widths of the wear facets, which would need to be further analyzed, or to an inaccuracy of using weight loss to determine wear resistance. However, the reasonable correlation between weight loss and wear depth suggests that the shape of the wear traces, which reflect the true volume loss, were different enough between groups that the simple measure of wear depth did not completely explain the differences in wear behavior between the materials. While overall wear of the appliance from volume measurements may be a concern, it is more likely that wear in a specific area which could lead to a hole being formed and enabling direct tooth to tooth contact may be

the most practical concern for the materials tested in this study. Thus, maximum wear depth was the measurement considered to be most important.

The correlation between hardness and wear depth (Fig. 12) was fitted with a second order polynomial with highly significant correlation ( $R^2= 0.94$ ). A direct relationship is observed with the hardest material tested, Endure (PVC), having the deepest wear, followed by the PECs in the middle, and then the PPCs being the softest and having the smallest wear depth. Traditionally an indirect relationship is observed between hardness and wear, with less loss due to wear as hardness increases, however a correlation similar to that shown in this study has been observed with different materials including alloys<sup>21,22</sup>. This observation could possibly be due the material flexing during testing, or to an elastic deformation produced during abrasion of the softer materials causing them to dissipate the energy of the moving antagonist as the abrader slides across the surface of the material but without material removal. In contrast, the harder materials do not flex or deform as much when the abrader slides across the surface causing more of the force to be used in the tearing process, leading to a direct loss of material from the surface.

SEM imaging of the unworn surfaces of Endure (PVC), C+ (PPC), and Ultra (PEC) (Fig. 13 A-C) show that Endure had the most irregular unworn surface, followed by C+, then Ultra. This is representative of the clinical look and clarity of these materials as Ultra, along with other PECs, are optically more transparent, with PPC and PVC being more opaque. The wear facet on Endure showed evidence of significant scratching, tearing and lifting of the material (Fig. 14 C). This suggests not only an abrasive force but quite possibly a significant frictional force as well. In comparison, Ultra and C+ (Fig. 14 A,B) exhibit less tearing of the material with C+ showing the

least. Fig. 15 A-C demonstrates the extent of the tearing and lifting along the facet at a greater magnification. The lifting and tearing is most likely resultant from an increase of frictional force and the hardness of these materials, as well as initial surface roughness. It is hypothesized that due to the decreased Vickers hardness of these materials, which may equate to less rigidity, there is more elastic deformation when the abrader is slid across the surface. This elastic deformation, rather than the plastic deformation of tearing, could possibly be the mechanism of resistance to the force of wear and would justify the direct correlation noted between hardness and wear depth (Fig. 12) with Endure being the hardest material with the greatest wear depth, followed by PECs and PPCs with C+ having the lowest hardness value and shallowest facets. It is also possible that the rougher initial surface of Endure (Fig. 13 C) caused it to have greater wear as compared with the smoother surfaces of the other materials, possibly due to greater frictional forces on the material exposed to the abrader due to it being raised above the surface, and making it more easily abraded off.

The parameters of this experiment were slightly altered from Gardner et al. and Raja et al.'s protocols<sup>7,11</sup>. Gardner et al.<sup>11</sup> set the abrasive force at 245 N or 25 kg based on a previous study by Gibbs et al.<sup>23</sup>, which reported that during clenching forces ranged between 25 kg and 127 kg (245-1245 N). Raja et al.<sup>7</sup> on the other hand applied a force of 4.5 N or 460 g. Both cycled the abrader at 1,000 cycles per sample. The current study set the abrasive force at 45 N or 4.6 kg. This value was based on previous research that determined normal occlusal forces to range from 10-80 N<sup>23-27</sup>. In fact, Graf et al.<sup>28</sup> found the axial force on a single tooth to be around 4 kg or 40 N. 45 N appeared to be a good approximation of standard opening and closing forces

assuming no clenching or mastication associated with eating was taking place, as patients should not be eating while wearing their VFRs.

The cycle duration in this experiment was set at 2,500 cycles which allowed visualization of the facet with the laser profilometer and loss of enough material to acquire a weight loss measurement. If the facet became deeper as the case would be with increased cycles, there was a greater chance of wearing through the sample, making measurement of the wear depth inaccurate with the laser profilometer.

A total of six chambers (two per machine) were used to abrade the samples. The specimens were cycled in each of the six chambers twice to produce equal variances among the samples and eliminate any bias from using the same machine for all runs of a given material. Simply surveying the data, no trend for heightened wear in any specific chamber was detected, suggesting that although the individual loads were not all identical at 45 N, the variability was small enough that it did not affect the outcomes and bias the results in any specific chamber.

Attrition is defined as wear caused by tooth on tooth contact in the mouth, whereas abrasion occurs when foreign material on the tooth, acting as a third body, causes wear. In the typical chewing motion there is an abrasive force which is overcome by an increase in force to cause attrition<sup>20</sup>. The electronics of the OHSU oral wear simulator are capable of producing both a lower abrasion and higher attrition force within the same wear trace. However, for this study, a single force was used, maintaining a stable 45 N force against the sample, and no third body was interposed because wear of a VFR is expected to occur from direct contact of tooth on the appliance material in saliva.

Choosing a standardized material for the antagonist abrader has sparked discussion and disagreement among many researchers. One would consider enamel to be the ideal abrader, however there are many difficulties associated with using this material. Standardization of enamel abrader shape is difficult to accomplish<sup>29</sup>, the hardness of superficial and deep enamel as well as superficial and deep dentin are significantly different and could produce variability in results<sup>29</sup>, and natural human cusps are difficult to harvest in large quantities<sup>30</sup>. Steatite ceramic spheres have also been advocated as enamel replacement antagonist abraders due to their ease of standardization, hardness that is similar to enamel, and well correlated wear rates and coefficients of friction in comparison to enamel<sup>31</sup>. Other researchers have opposed the use of steatite claiming this material has higher hardness than enamel<sup>30,32</sup>. These authors have suggested the use of IPS Empress classic ceramic (Ivoclar), claiming that it has similar wear and other tribological characteristics to enamel<sup>30,32</sup>. This study utilized steatite spheres as the abrader for the benefits listed above and to attempt to follow the protocols of previous studies<sup>7,11</sup>. However, this study used 6.5 mm diameter spheres, whereas Gardner et al.<sup>11</sup> utilized 8 mm spheres and Raja et al.<sup>7</sup> 9.5 mm spheres. Smaller spheres were selected to try to emulate the smaller size of cusps found in natural dentition. The disadvantage of using the smaller spheres was forming wear traces with steep walls, which proved to be difficult to image with the laser profilometer. The laser would refract from the wall rather than reflect back to profilometer sensor, causing optical burnout of the images. Perhaps using a larger diameter sphere would create more gradual inclines of the wear trace walls and allow easier imaging of the wear traces.



It is difficult to compare the results of the previous studies by Gardner et al.<sup>11</sup> and Raja et al.<sup>7</sup> with the results of this experiment because each study employed a different machine to test the wear resistance of the materials. Furthermore, the authors used different protocols in terms of force and number of cycles of abrasion. Regardless, the results of this study are starkly different from previous studies and warrant a closer evaluation of wear resistance of various PPC and PECs.

## **Conclusions:**

The results of this experiment lead to the rejection of the null hypothesis that there is no difference in wear resistance between the materials. The conclusions obtained are the following:

- Endure (PVC) had the greatest wear depth of all of the materials, and Ultra (PEC) had greater wear depth than the PPC group (C+ and Invisacryl C). The remaining PECs (Ace and Plus) did not differ statistically from the PPCs.
- Endure (PVC) had greater weight loss than the PPC group (C+ and Invisacryl C). The PECs (Ace, Ultra and Plus) and PPCs were not statistically different.
- There is a direct linear correlation between weight loss and wear depth with Endure (PVC) having the greatest wear depth and weight loss, and PPCs (C+ and Invisacryl C) losing the least.
- There is a direct correlation between hardness and wear depth.
- There is no difference in calculated volume loss between the groups.

## References:

1. Littlewood SJ, Millett DT, Doubleday B, Bearn DR, Worthington HV. **Retention procedures for stabilising tooth position after treatment with orthodontic braces.** *Cochrane Database Syst Rev.* 2004;(1)(1):CD002283
2. Littlewood SJ, Mitchell L. *Retention. An introduction to orthodontics.* 4th ed. Oxford University Press; 2013.
3. Melrose C, Millett DT. **Toward a perspective on orthodontic retention?** *American Journal of Orthodontics and Dentofacial Orthopedics.* 1998;113(5):507K514.
4. Proffit WR, Fields HW, and Sarver DM. *Contemporary Orthodontics.* 5th ed. St. Louis: Mosby, 2013.
5. Little RM, Riedel RA, Artun J. **An evaluation of changes in mandibular anterior alignment from 10 to 20 years post-retention.** *American Journal of Orthodontics and Dentofacial Orthopedics.* 1988;93(5):423K428.
6. Ponitz RJ. **Invisible retainers.** *American Journal of Orthodontics and Dentofacial Orthopedics.* 1971;59(3):266K272.
7. Raja TA, Littlewood SJ, Munyombwe T, Bubb NL. **Wear resistance of four types of vacuum formed retainer materials: A laboratory study.** *Angle Orthod.* 2014; 84(4):656K664.

8. McNamara JA, Kramer KL, Juenker JP. **Invisible retainers.** *J Clin Orthod.* 1985;19(8):570K578.
9. Wang F. **A new thermoplastic retainer.** *J Clin Orthod.* 1997;31(11):754K757.
10. Sheridan JJ, LeDoux W, McMinn R. **Essix retainers: Fabrication and supervision for permanent retention.** *J Clin Orthod.* 1993;27(1):37K45.
11. Gardner GD, Dunn WJ, Taloumis L. **Wear comparison of thermoplastic materials used for orthodontic retainers.** *American Journal of Orthodontics and Dentofacial Orthopedics.* 2003;124(3):294K297.
12. Mai W, He J, Jiang Y, Huang C, Li M, Yuan K, Kang N, **Comparison of vacuum-formed and Hawley retainers: a systematic review,** *American Journal of Orthodontics and Dentofacial Orthopedics;* 145 (6), pp. 720-727
13. Sun J, Yu YC, Liu MY, Chen L, Li HW, Zhang L, Zhou Y, Ao D, Tao R, Lai WL, **Survival Time Comparison between Hawley and Clear Overlay Retainers: A Randomized Trial,** *J Dent Res*
14. Rowland H, Hichens L, Williams A, et al. **The effectiveness of Hawley and vacuum formed retainers: A single center randomized controlled trial.** *American Journal of Orthodontics and Dentofacial Orthopedics.* 2007;132(6):730K737.
15. Hichens L, Rowland H, Williams A, et al. **Cost-effectiveness and patient satisfaction: Hawley and vacuum-formed retainers.** *The European Journal of Orthodontics.* 2007;29(4):372K378.

16. Mollov ND, Lindauer SJ, Best AM, Shroff B, Tufekci E, **Patient attitudes toward retention and perceptions of treatment success.**, *Angle Orthod.* 2010 Jul;80(4):468-73. doi: 10.2319/102109-594.1.
17. Sheridan JJ, Armbruster P. **Bleaching teeth during supervised retention.** *J Clin Orthod.* 1999;33(6):339K344.
18. Sauget E, Covell DA, Boero RP, Lieber WS. **Comparison of occlusal contacts with use of hawley and clear overlay retainers.** *Angle Orthod.* 1997;67(3):223K230.
19. Pascual AL, Beeman CS, Hicks EP, Bush HM, Mitchell RJ. **The essential work of fracture of thermoplastic orthodontic retainer materials.** *Angle Orthod.* 2010;80(3):554K561.
20. Condon, Ferracane JL, **Evaluation of composite wear with a new multi-mode oral wear simulator** *Dent Mater*, 12 (1996), pp. 218–226
21. Jeong DH , Erb U , Aust KT , Palumbo G. **The relationship between hardness and abrasive wear resistance of electrodeposited nanocrystalline Ni–P coatings** *Scripta Materialia* 2003; 48:1067–1072
22. Qian L, Xiao X, Sun Q, Yu T. **Anomalous relationship between hardness and wear properties of a superelastic nickel–titanium alloy.** *Appl. Phys. Lett.*, Vol. 84, No. 7, 16 February 2004

23. Gibbs CH, Mahan PE, Lundeen HC, Brehnan K, Walsh EK, Holbrook. **Occlusal forces during chewing and swallowing as measured by sound transmission.** *J Prosthet Dent* 1981;46:443-9
24. Gibbs CH, Mahan PE, Lundeen HC, Brehnan K, Walsh EK, Sinkewiz SL, Ginsberg SB. **Occlusal forces during chewing- influences of biting strength and food consistency.** *J Prosthet Dent* 1981; 46:561-7
25. Bates JF, Stafford GD, Harrison A. **Masticatory function- A review of literature.** *J Oral Rehabil* 1975;2:349
26. De Gee AJ, Pallav P, Davidson CL. **Effect of abrasion medium on wear of stress-bearing composites and amalgam in-vitro.** *J Dent Res* 1986;65:654-8
27. Sakaguchi RL, Douglas WH, DeLong R, Pintado MR. **The wear of posterior composite in an artificial mouth: a clinical correlation.** *Dent Mater* 1986;2:235-240
28. Graf H, Grassl H, Aeberhard HJ. **A method of measurement of occlusal forces in three dimensions.** *Helv Odontol Acta* 1974; 18:7
29. Zheng J; Zhou ZR; Zhang J; Li H; Yu Y; **On the friction and wear behavior of human tooth enamel and dentin.** *Wear* 2003; 255:967-974)
30. Krejci I, Albert P, and Lutz P; **The Influence of Antagonist Standardization on Wear.** *JDR* February 1999 vol. 78 no. 2 713-719)

31. Wassel RW, McCabe JF, Walls AWK, **Wear characteristics in a two-body wear test Dental Materials**, 10 (1994), pp. 269–274
  
32. Shortall AC, Hu XQ, Marquis PM. **Potential countersample materials for in-vitro simulation wear testing.** *Dent Mater.*2002;18:246–254

## Figure Legends:

**FIGURE 1:** Profilometer imaging of Ace. **A.** shows the wear facet with color coding of the topography of the facet, **B.** is a stylized image of the facet, **C.** is a cross section of the deepest point of the facet. Two horizontal lines are placed on the cross sectional image, one at the deepest portion of the wear facet and the other at a point obtained from averaging the unworn boundaries around the facet. The green vertical streaks represent areas in which data collection was interrupted (lost) due to some surface feature that the laser could not reflect from.

**FIGURE 2:** Profilometer imaging of Plus. **A.** shows the wear facet with color coding of the topography of the facet, **B.** is a stylized image of the facet, **C.** is a cross section of the deepest point of the facet. Two horizontal lines are placed on the cross sectional image, one at the deepest portion of the wear facet and the other at a point obtained from averaging the unworn boundaries around the facet. The green vertical streaks represent areas in which data collection was interrupted (lost) due to some surface feature that the laser could not reflect from.

**FIGURE 3:** Profilometer imaging of Ultra. **A.** shows the wear facet with color coding of the topography of the facet, **B.** is a stylized image of the facet, **C.** is a cross section of the deepest point of the facet. Two horizontal lines are placed on the cross sectional image, one at the deepest portion of the wear facet and the other at a point obtained from averaging the unworn boundaries around the facet. The green vertical streaks represent areas in which data collection was interrupted (lost) due to some surface feature that the laser could not reflect from.

**FIGURE 4:** Profilometer imaging of Endure. **A.** shows the wear facet with color coding of the topography of the facet, **B.** is a stylized image of the facet, **C.** is a cross section of the deepest point of the facet. Two horizontal lines are placed on the cross sectional image, one at the deepest portion of the wear facet and the other at a point obtained from averaging the unworn boundaries around the facet. The green vertical streaks represent areas in which data collection was interrupted (lost) due to some surface feature that the laser could not reflect from.

**FIGURE 5:** Profilometer imaging of C+. **A.** shows the wear facet with color coding of the topography of the facet, **B.** is a stylized image of the facet, **C.** is a cross section of the deepest point of the facet. Two horizontal lines are placed on the cross sectional image, one at the deepest portion of the wear facet and the other at a point obtained from averaging the unworn boundaries around the facet. The green vertical streaks represent areas in which data collection was interrupted (lost) due to some surface feature that the laser could not reflect from.

**FIGURE 6:** Profilometer imaging of Invisacrlyl. **A.** shows the wear facet with color coding of the topography of the facet, **B.** Is a stylized image of the facet, **C.** is a cross section of the deepest point of the facet. Two horizontal lines are placed on the cross sectional image, one at the deepest portion of the wear facet and the other at a point obtained from averaging the unworn boundaries around the facet. The green vertical streaks represent areas in which data collection was interrupted (lost) due to some surface feature that the laser could not reflect from.

**FIGURE 7:** Barber-Colman conversion curves for GYZ-934-1 Impressor portable hardness tester.



**FIGURE 8:** Graph of average maximum depth loss of each sample. Red groups are PECs, blue is PVC, and grey/black are PPCs. \* Denotes the Endure demonstrated a significantly greater wear depth when compared to all other groups. \*\* Denotes Ultra having greater wear depth than C+ and Invisacryl C.

**FIGURE 9:** Graph of average net weight loss of each sample post desiccation. Red groups are PECs, blue is PVC, and grey/black are PPCs. \* Denotes the Endure demonstrated a significant net weight loss when compared to C+ and Invisacryl C.

**FIGURE 10:** Correlation of average weight loss with average maximum wear depth for each material. Red groups are PECs, blue is PVC, and grey/black are PPCs. The linear trend line has an  $R^2 = 0.87$  representing a significant correlation between weight and wear depth.

**FIGURE 11:** Graph of average volume loss of each sample. Red groups are PECs, blue is PVC, and grey/black are PPCs. No statistically significant difference was found between any of the groups.

**FIGURE 12:** Correlation of Vickers hardness with average maximum wear depth for each material. Red groups are PECs, blue is PVC, and grey/black are PPCs. The second order polynomial trend line has an  $R^2 = 0.94$  representing a significant direct relationship between hardness and depth loss.

**FIGURE 13:** **A.** SEM image of the unworn surface of Ultra at 500x magnification, **B.** SEM image of the unworn surface of C+ at 500x magnification, **C.** SEM image of the unworn surface of Endure at 500x magnification.

**FIGURE 14:** **A.** SEM image of the worn surface of Ultra at 500x magnification, **B.** SEM image of the worn surface of C+ at 500x magnification, **C.** SEM image of the worn surface of Endure at 500x magnification.

**FIGURE 15:** **A.** SEM image of the worn surface of Ultra at 1750x magnification, **B.** SEM image of the worn surface of C+ at 1750x magnification, **C.** SEM image of the worn surface of Endure at 1750x magnification

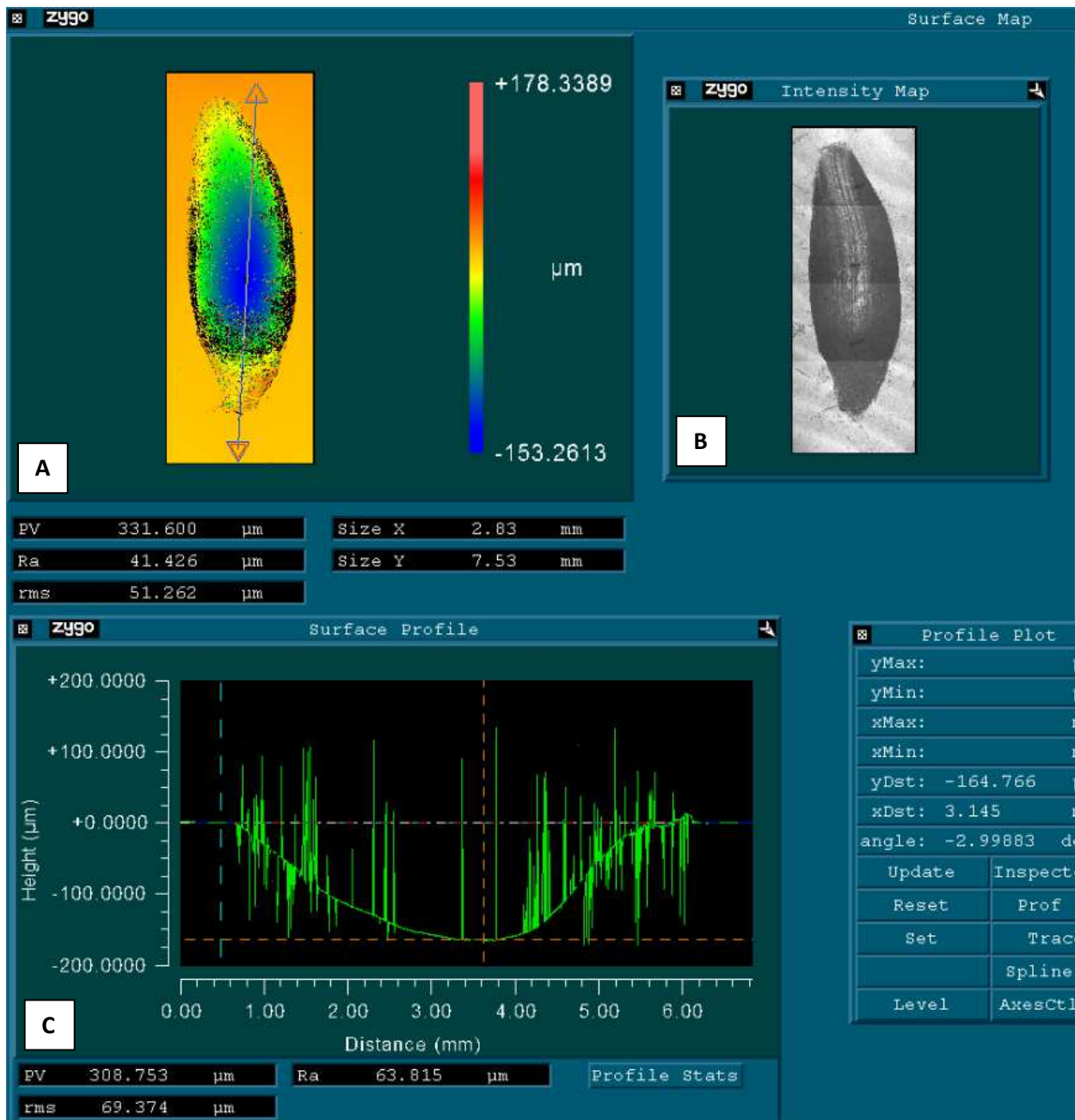


**Figure 1**

Profilometer imaging of Ace. **A.** shows the wear facet with color coding of the topography of the facet, **B.** is a stylized image of the facet, **C.** is a cross section of the deepest point of the facet. Two horizontal lines are placed on the cross sectional image, one at the deepest portion of the wear facet and the other at a point obtained from averaging the unworn boundaries around the facet. The green vertical streaks represent areas in which data collection was interrupted (lost) due to some surface feature that the laser could not reflect from.

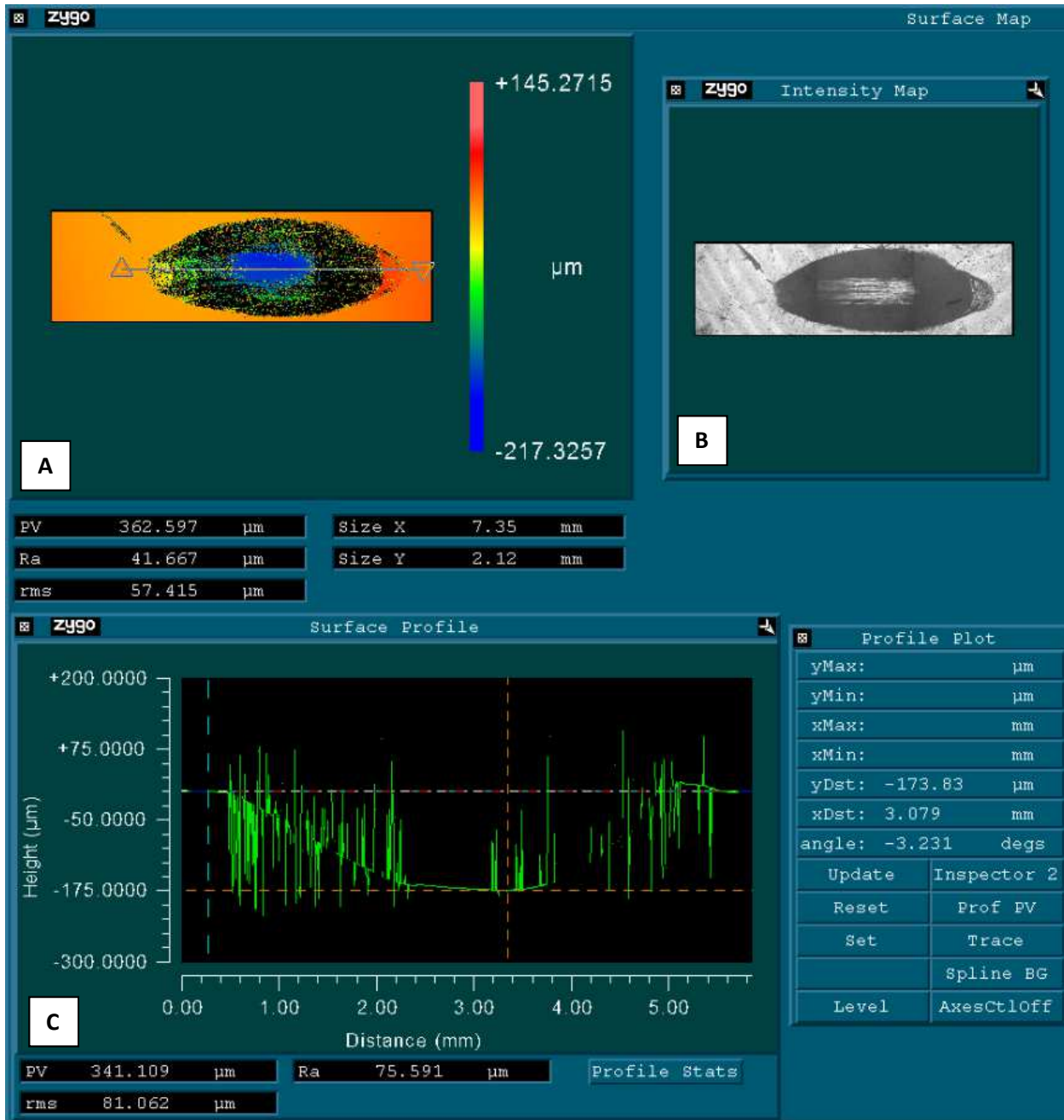


**Figure 2**

Profilometer imaging of Plus. **A.** shows the wear facet with color coding of the topography of the facet, **B.** is a stylized image of the facet, **C.** is a cross section of the deepest point of the facet. Two horizontal lines are placed on the cross sectional image, one at the deepest portion of the wear facet and the other at a point obtained from averaging the unworn boundaries around the facet. The green vertical streaks represent areas in which data collection was interrupted (lost) due to some surface feature that the laser could not reflect from.

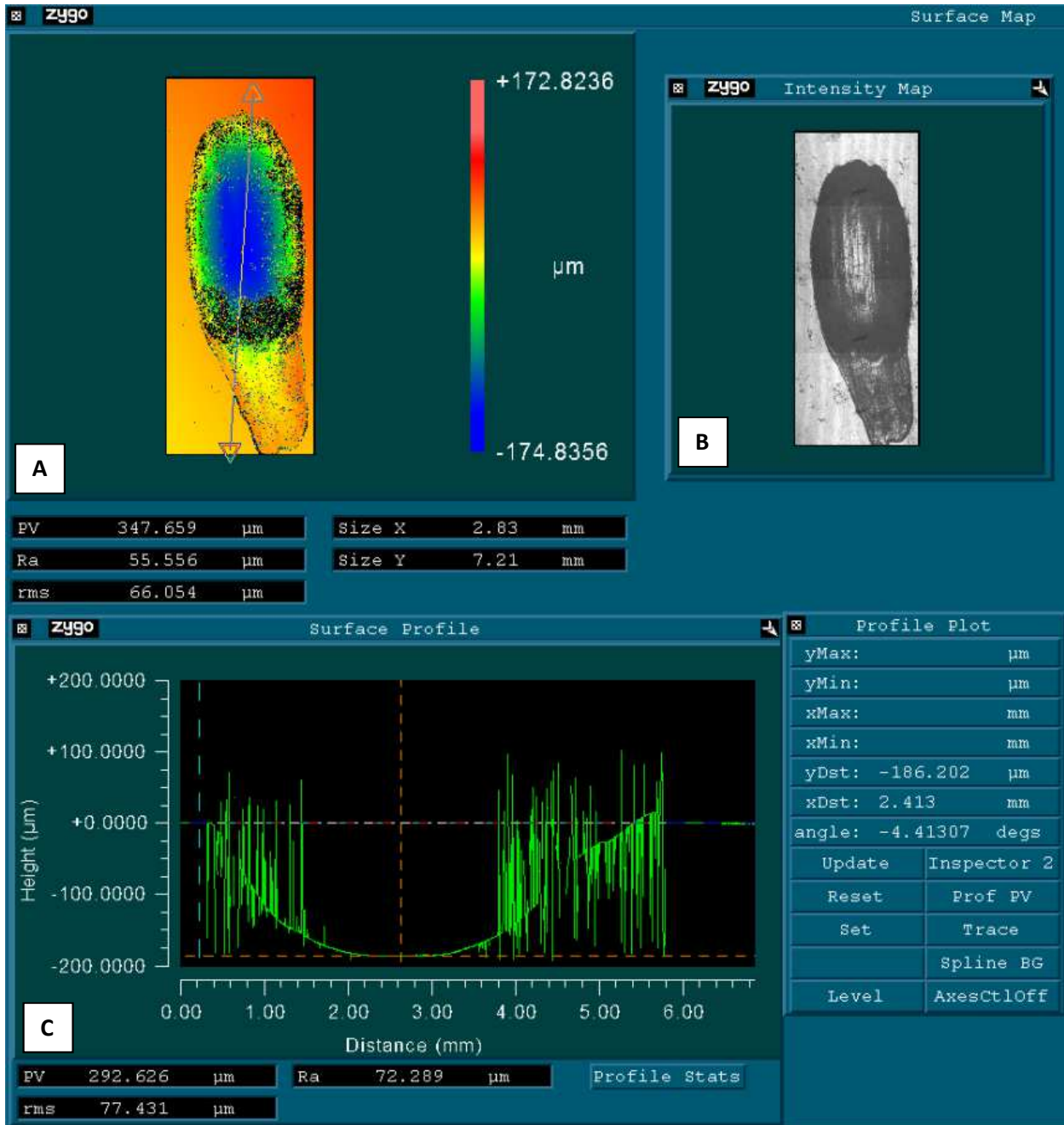


**Figure 3**

Profilometer imaging of Ultra. **A.** shows the wear facet with color coding of the topography of the facet, **B.** is a stylized image of the facet, **C.** is a cross section of the deepest point of the facet. Two horizontal lines are placed on the cross sectional image, one at the deepest portion of the wear facet and the other at a point obtained from averaging the unworn boundaries around the facet. The green vertical streaks represent areas in which data collection was interrupted (lost) due to some surface feature that the laser could not reflect from.

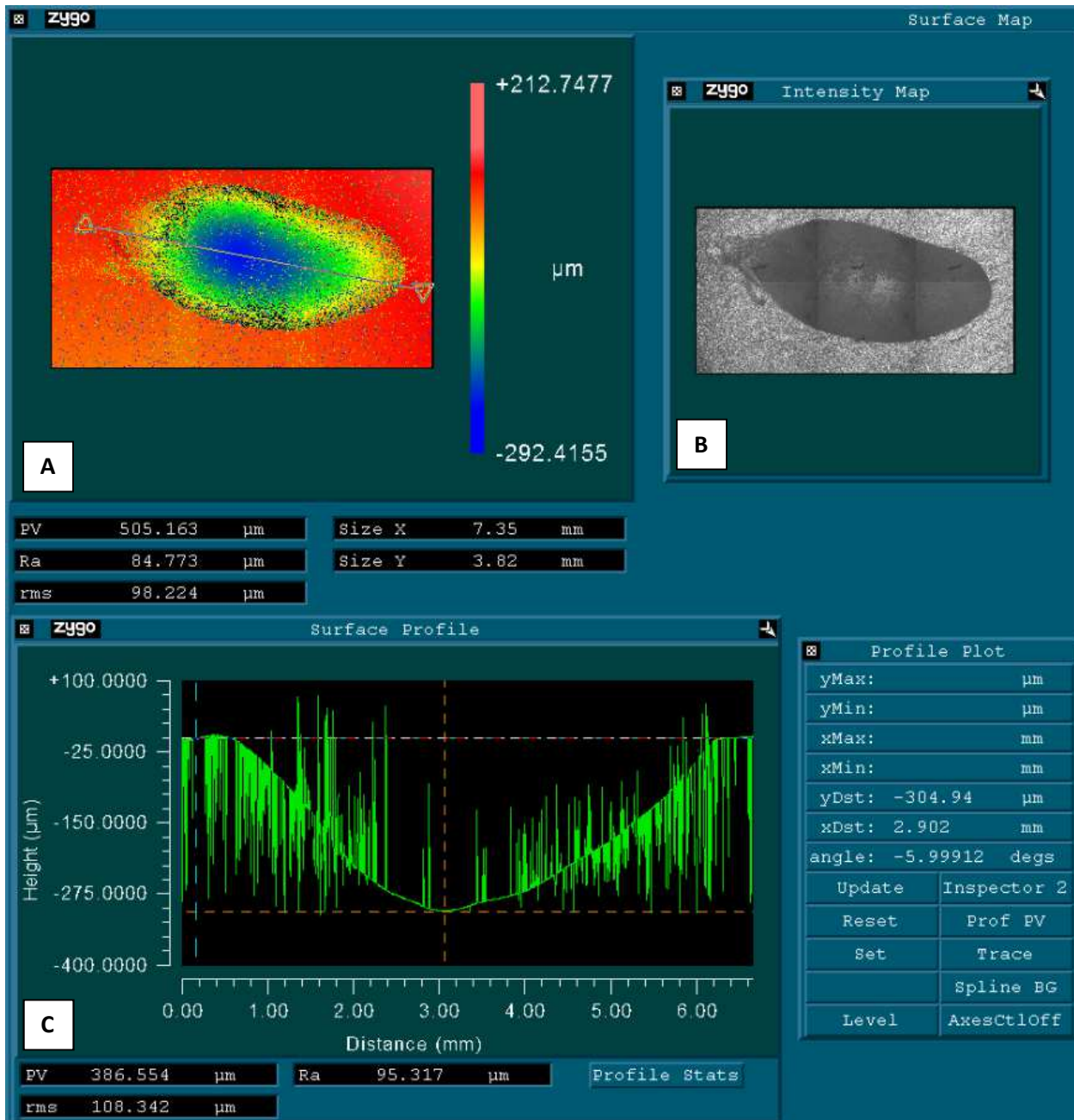


**Figure 4**

Profilometer imaging of Endure. **A.** shows the wear facet with color coding of the topography of the facet, **B.** is a stylized image of the facet, **C.** is a cross section of the deepest point of the facet. Two horizontal lines are placed on the cross sectional image, one at the deepest portion of the wear facet and the other at a point obtained from averaging the unworn boundaries around the facet. The green vertical streaks represent areas in which data collection was interrupted (lost) due to some surface feature that the laser could not reflect from.

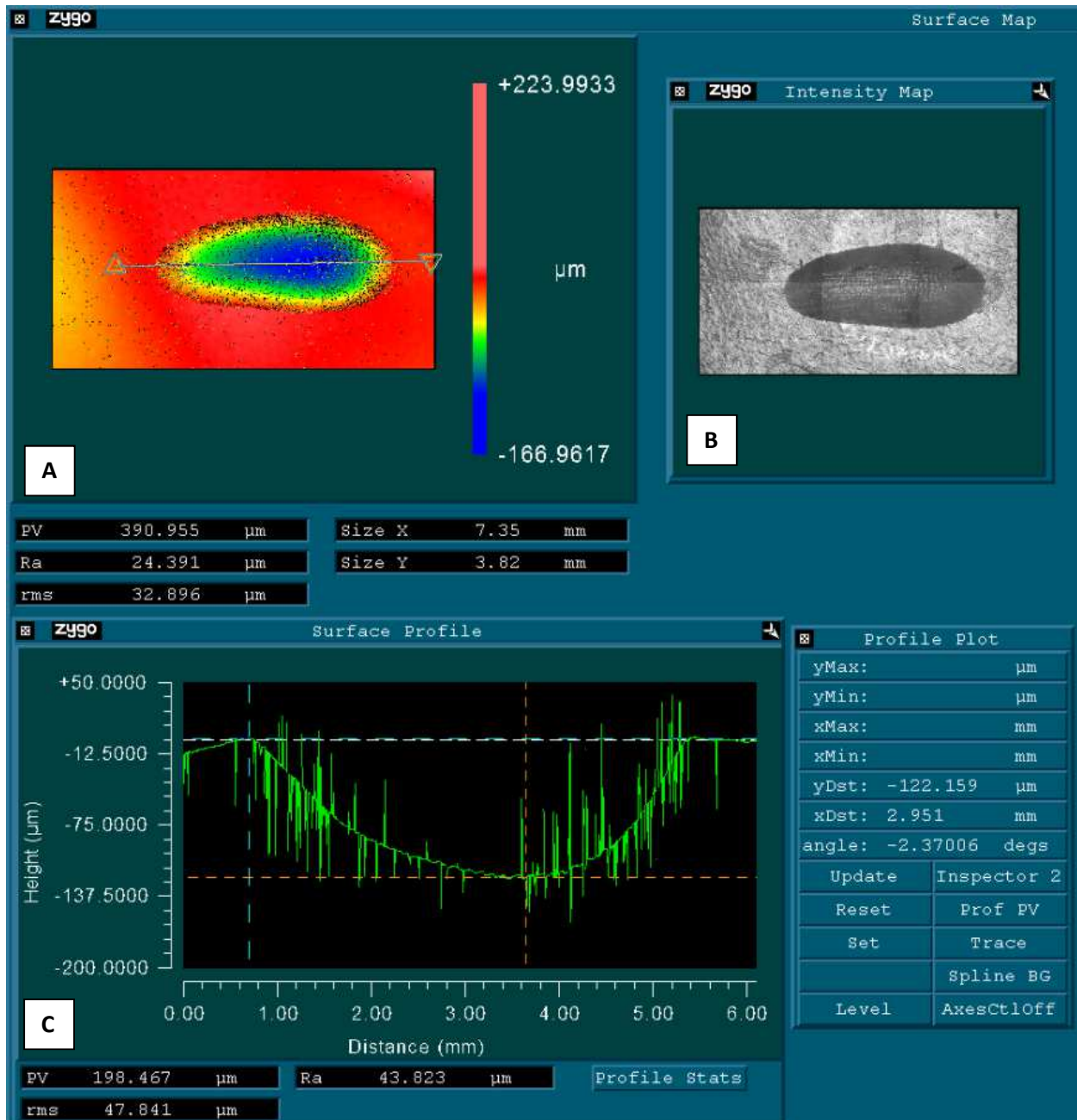


**Figure 5**

Profilometer imaging of C+. **A.** shows the wear facet with color coding of the topography of the facet, **B.** is a stylized image of the facet, **C.** is a cross section of the deepest point of the facet. Two horizontal lines are placed on the cross sectional image, one at the deepest portion of the wear facet and the other at a point obtained from averaging the unworn boundaries around the facet. The green vertical streaks represent areas in which data collection was interrupted (lost) due to some surface feature that the laser could not reflect from.

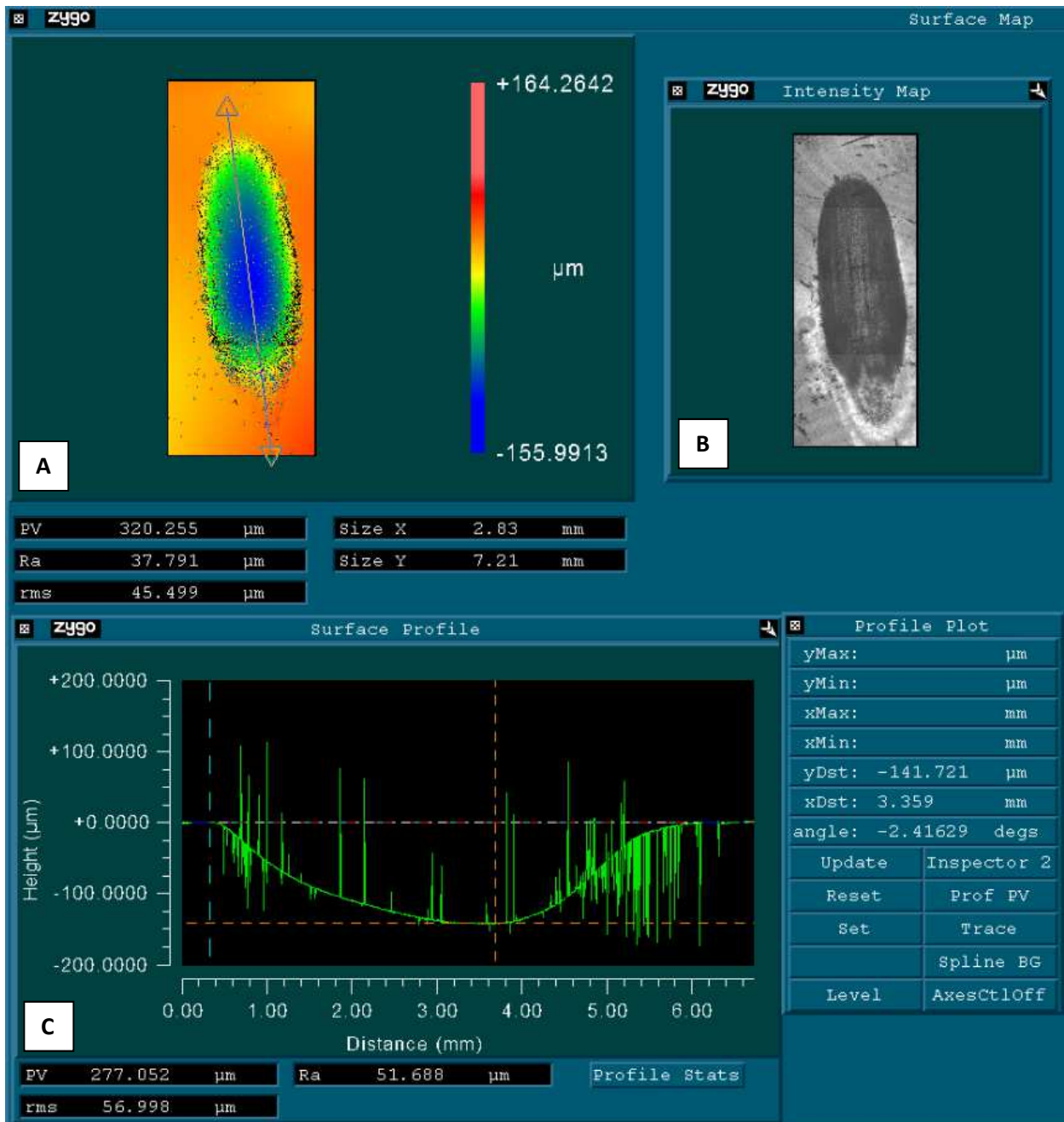


**Figure 6**

Profilometer imaging of Invisacryl. **A.** shows the wear facet with color coding of the topography of the facet, **B.** is a stylized image of the facet, **C.** is a cross section of the deepest point of the facet. Two horizontal lines are placed on the cross sectional image, one at the deepest portion of the wear facet and the other at a point obtained from averaging the unworn boundaries around the facet. The green vertical streaks represent areas in which data collection was interrupted (lost) due to some surface feature that the laser could not reflect from.



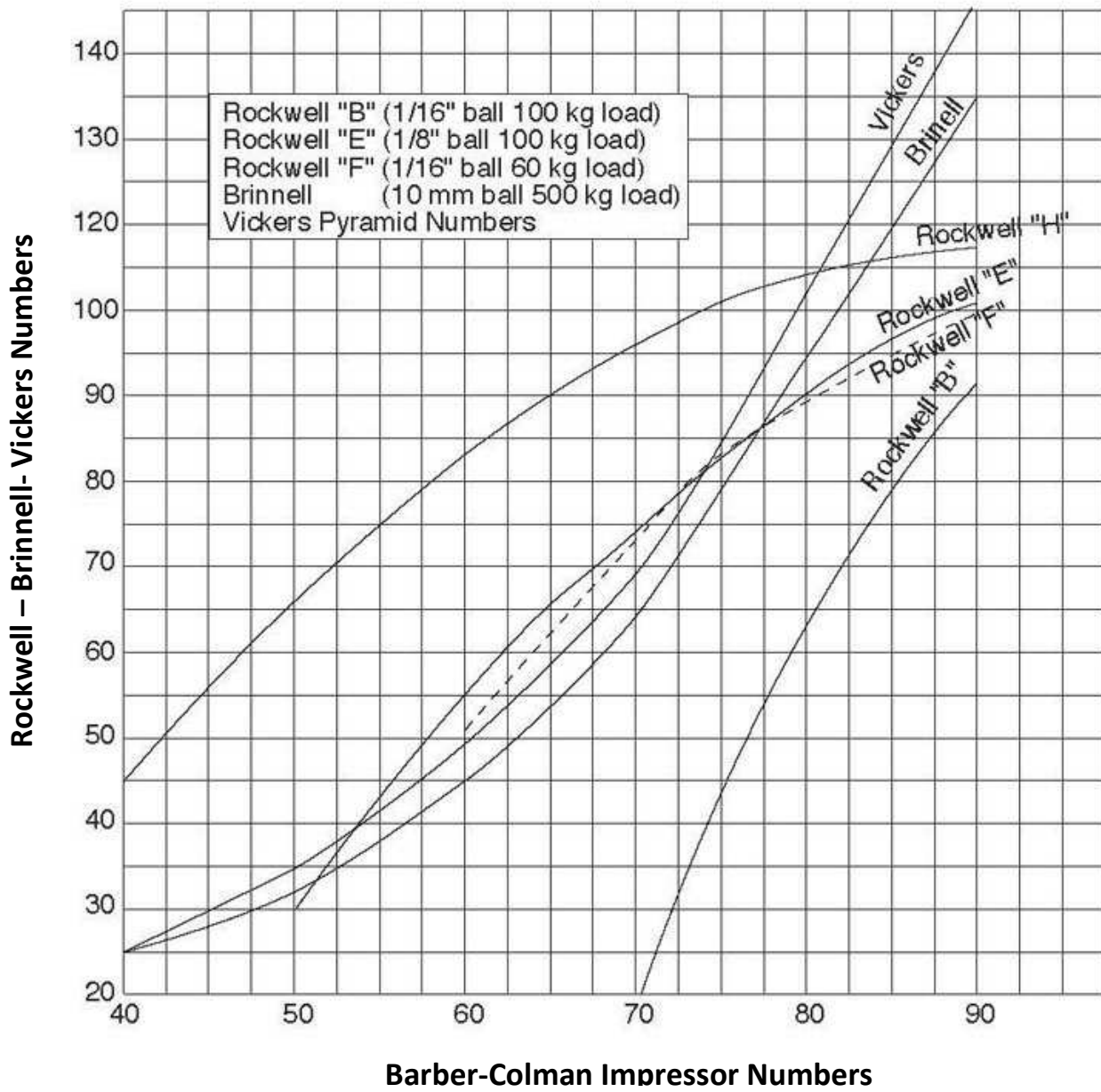


**Figure 7**

Barber-Colman conversion curves for GYZ-934-1 Impressor portable hardness tester.

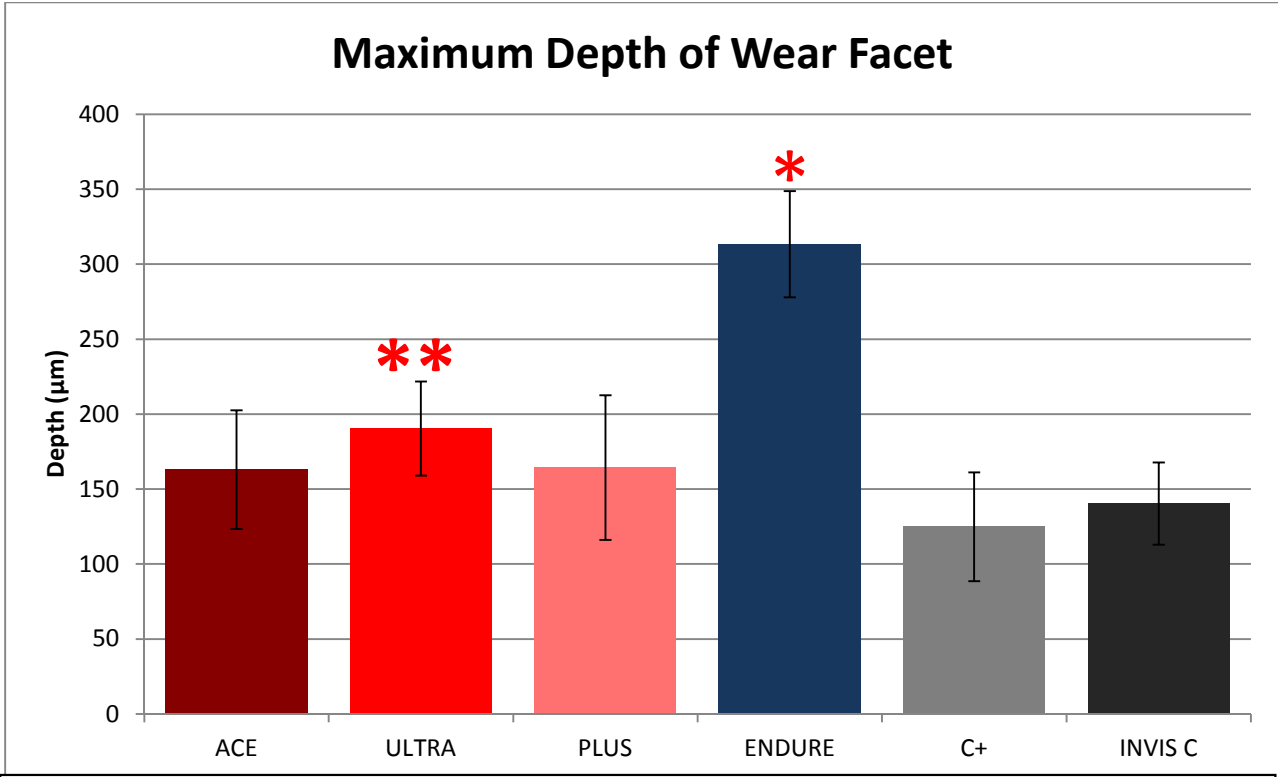


**Figure 8**

Graph of average maximum depth loss of each sample. Red groups are PECs, blue is PVC, and grey/black are PPCs. \* Denotes the Endure demonstrated a significantly greater wear depth when compared to all other groups. \*\* Denotes Ultra having greater wear depth than C+ and Invisacryl C.

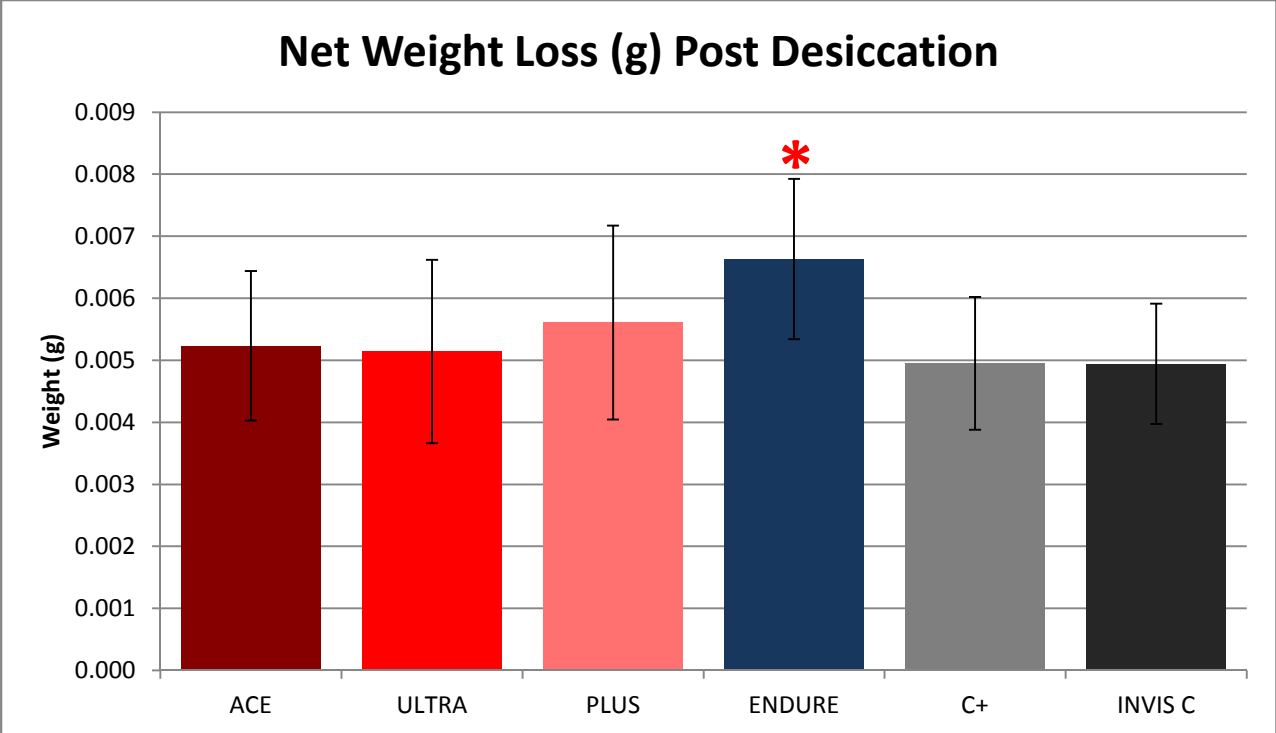


**Figure 9**  
Graph of average net weight loss of each sample post desiccation. Red groups are PECs, blue is PVC, and grey/black are PPCs. \* Denotes the Endure demonstrated a significant net weight loss when compared to C+ and Invisacrly C.



**Figure 10**

Correlation of average weight loss with average maximum wear depth for each material. Red groups are PECs, blue is PVC, and grey/black are PPCs. The linear trend line has an  $R^2 = 0.87$  representing a significant correlation between weight and wear depth. Both the PPC and PEC are in the lower third of the graph.

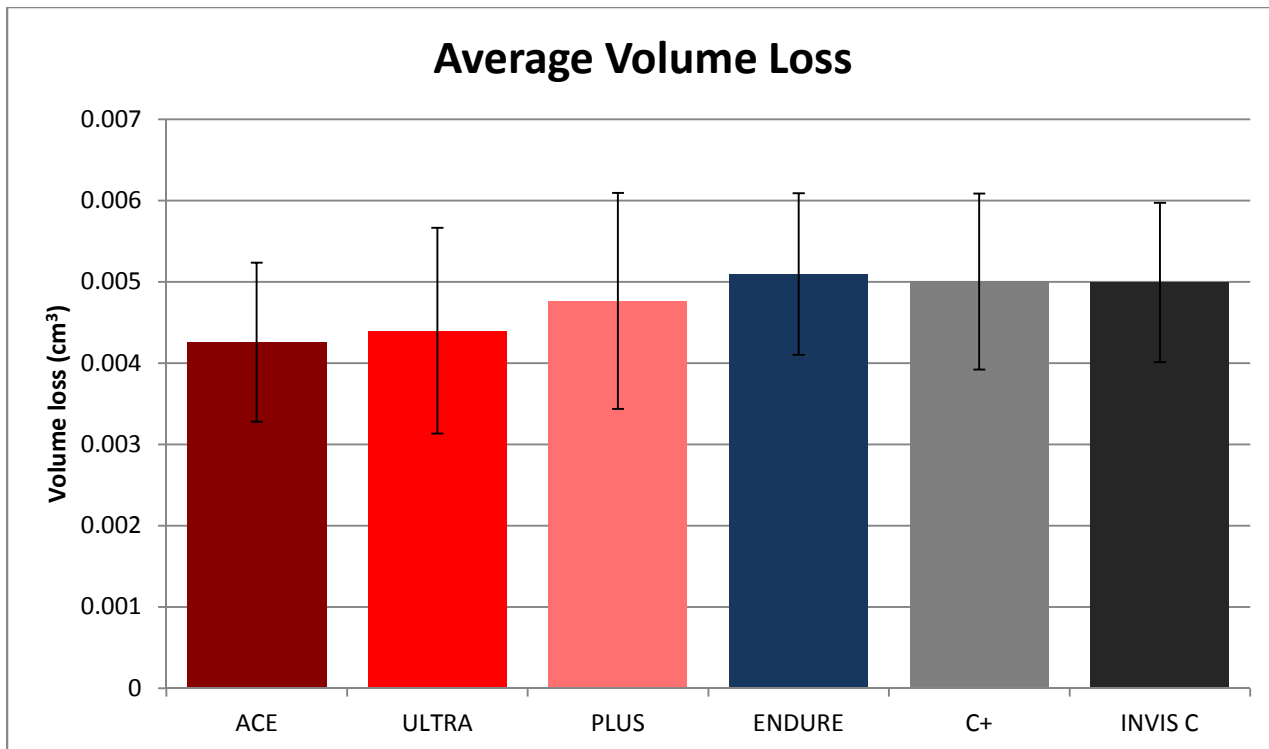


**Figure 11**

Graph of average volume loss of each sample. Red groups are PECs, blue is PVC, and grey/black are PPCs. No statistically significant difference was found between any of the groups.

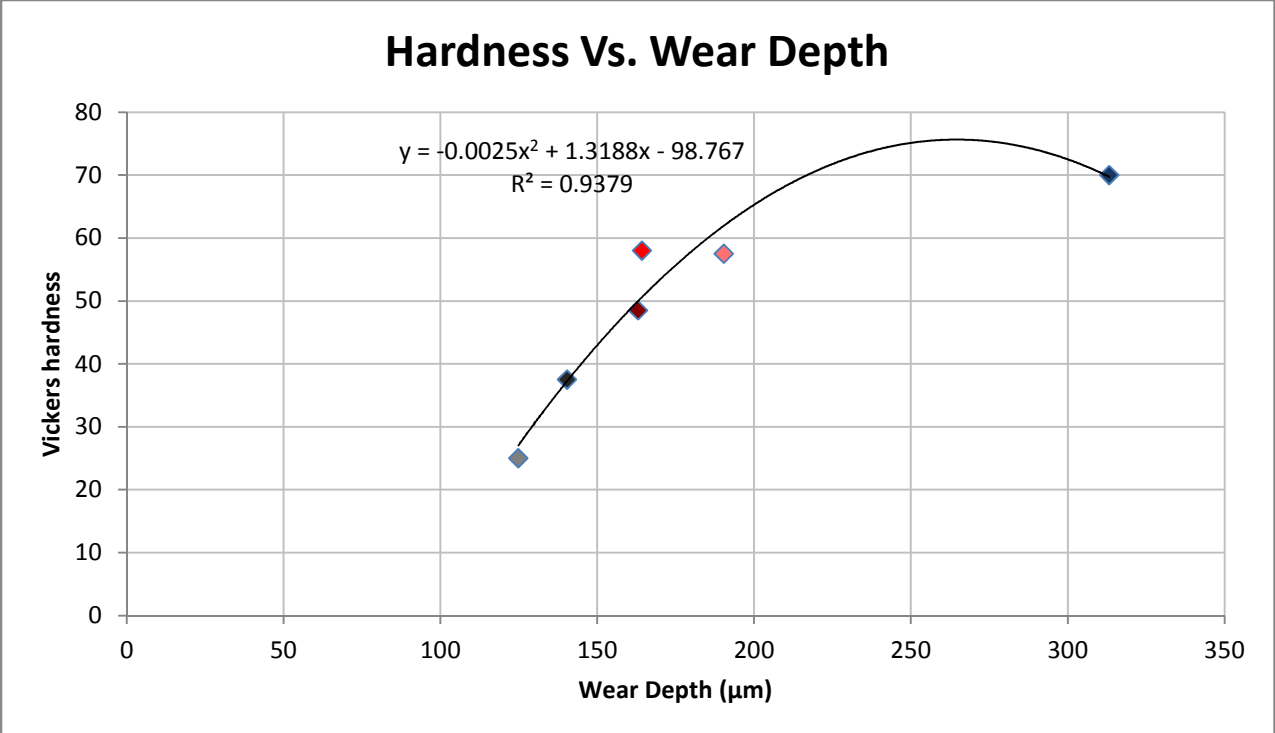


**Figure 12**

Correlation of Vickers hardness with average maximum wear depth for each material. Red groups are PECs, blue is PVC, and grey/black are PPCs. The second order polynomial trend line has an  $R^2 = 0.94$  representing a significant direct relationship between hardness and depth loss.

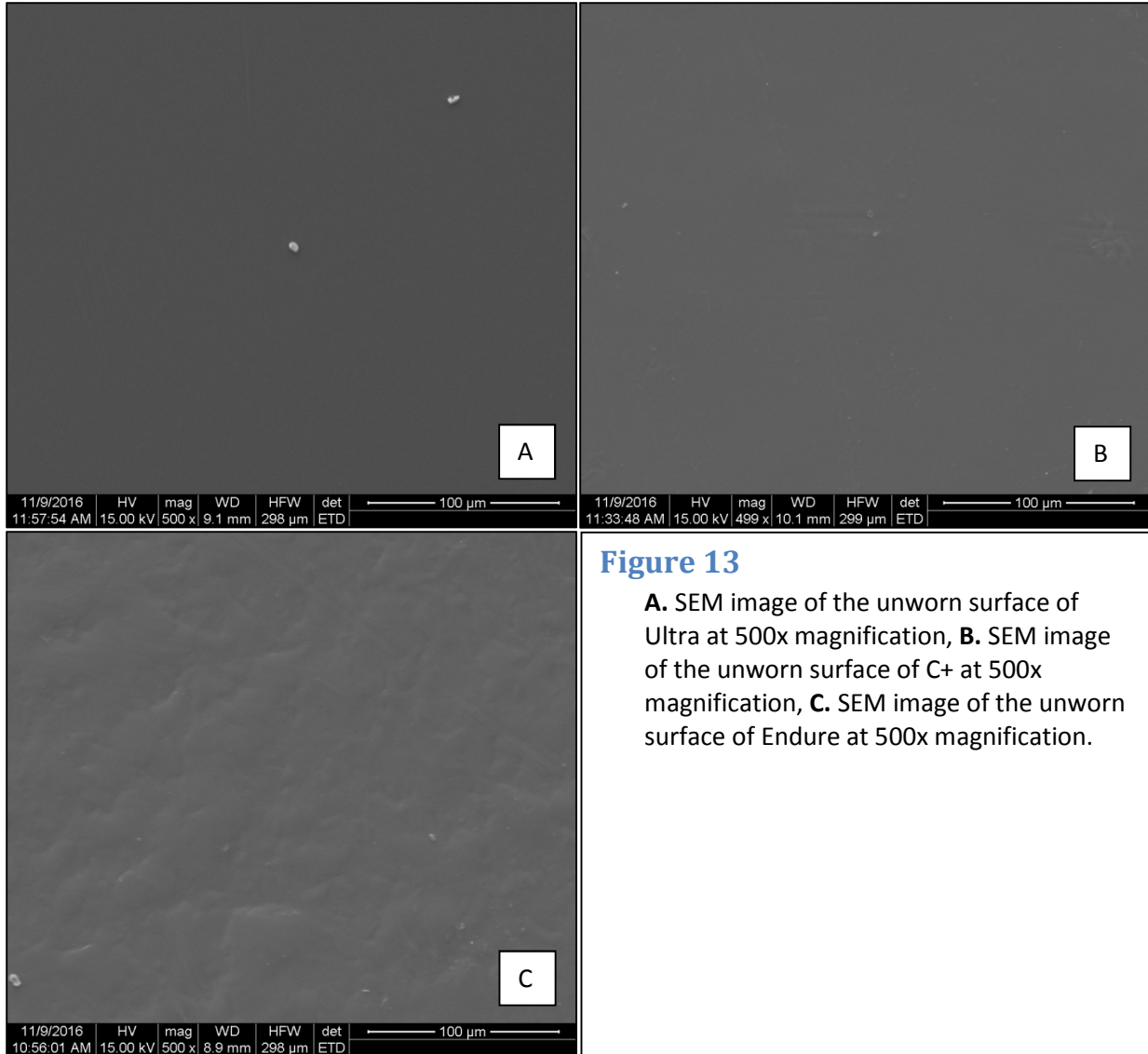


**Figure 13**

**A.** SEM image of the unworn surface of Ultra at 500x magnification, **B.** SEM image of the unworn surface of C+ at 500x magnification, **C.** SEM image of the unworn surface of Endure at 500x magnification.

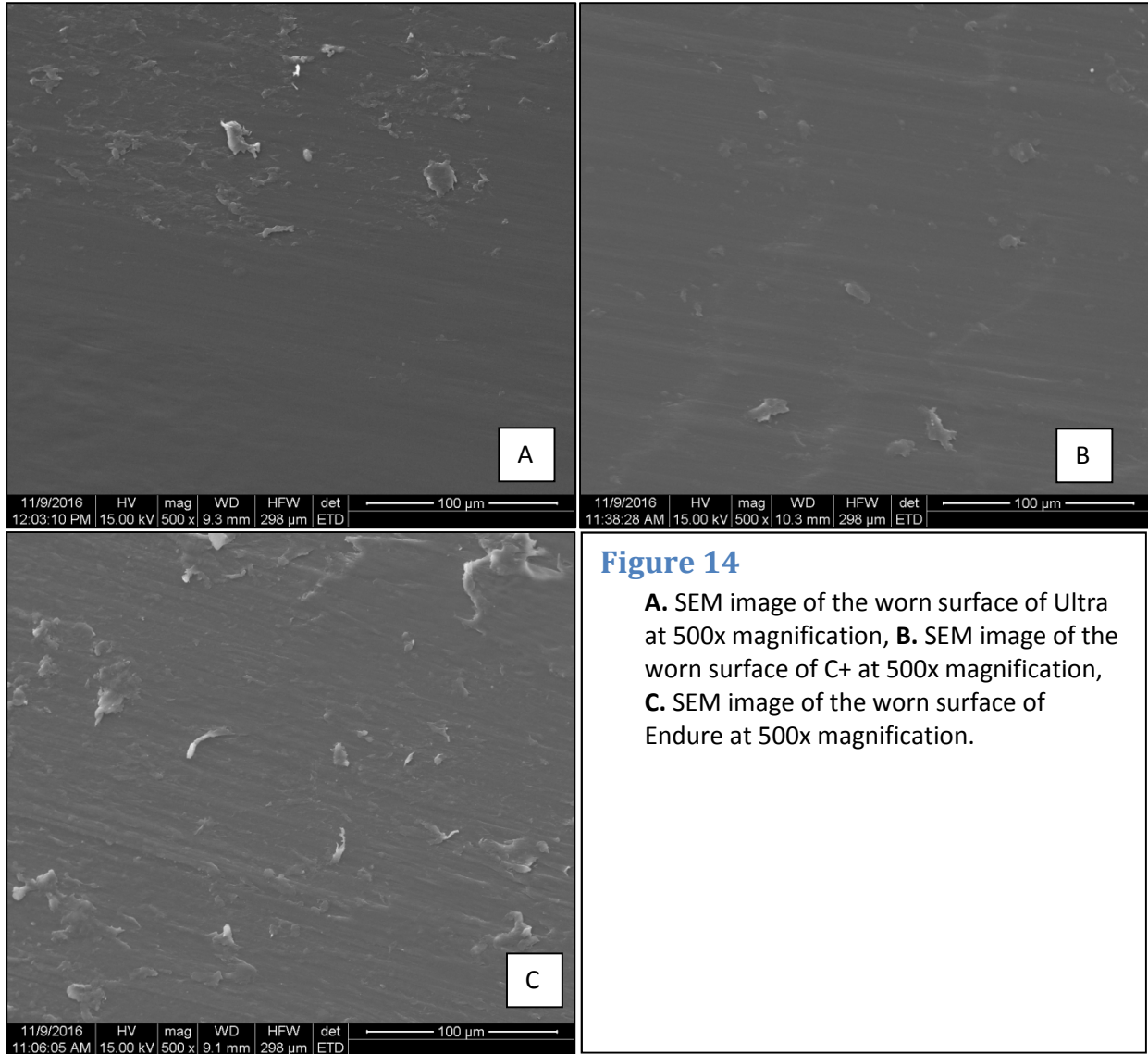


**Figure 14**

**A.** SEM image of the worn surface of Ultra at 500x magnification, **B.** SEM image of the worn surface of C+ at 500x magnification, **C.** SEM image of the worn surface of Endure at 500x magnification.



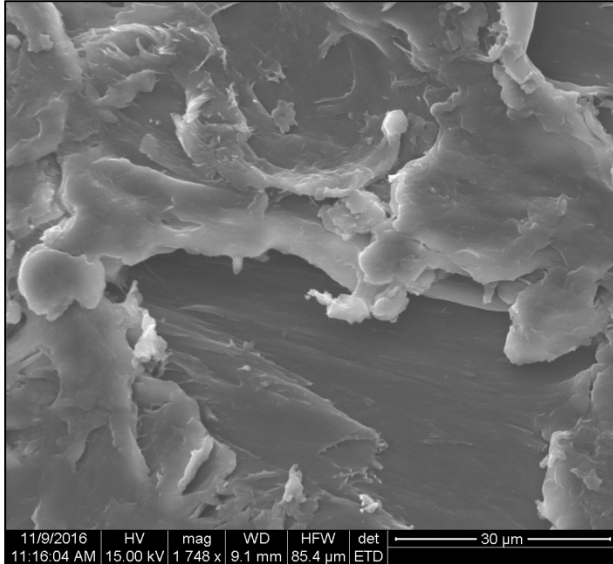
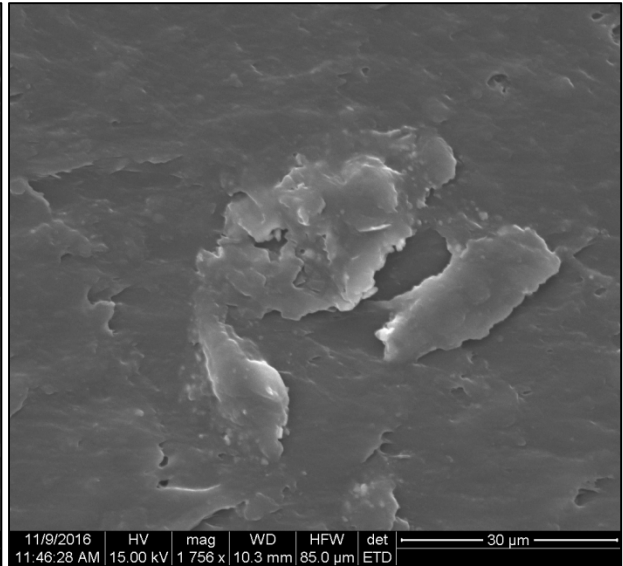
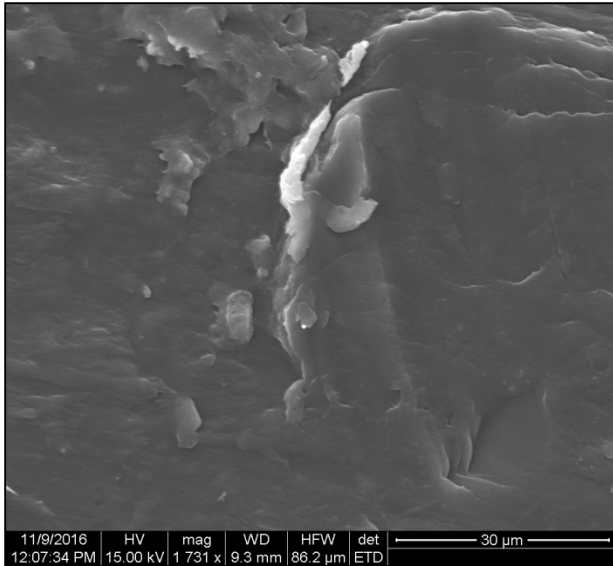


**Figure 15**

**A.** SEM image of the worn surface of Ultra at 1750x magnification, **B.** SEM image of the worn surface of C+ at 1750x magnification, **C.** SEM image of the worn surface of Endure at 1750x magnification.

## Table Legends:

**TABLE 1:** Material composition, heating time, Biostar code, and manufacturer.

**TABLE 2:** Densities and Vickers hardness values for each material. Red are PECs, Grey are PPC, and blue is PVC.

Composition	Material	Biostar Code	Heating Time	Manufacturer
polyethylene copolymers (PEC)	Ace	133	35	Raintree Essix
	Plus	143	40	Raintree Essix
	Ultra	153	45	Great Lakes Orthodontics
polypropylene copolymers (PPC)	C+	163	60	Raintree Essix
	Invis C	203	70	Great Lakes Orthodontics
polyvinyl chloride polymer (PVC)	Endure	132	35	Great Lakes Orthodontics

### Table 1

Material composition, heating time, Biostar code, and manufacturer.

Material	Vickers Hardness	Density g/cm <sup>3</sup>
Ace	48.5 ±0.4	1.225
Plus	58 ±0.3	1.181
Ultra	57.5±0.0	1.170
C+	25 ±0.3	0.994
Invis C	37.5 ±0.7	0.987
Endure	70 ±1.3	1.302

### Table 2

Densities and Vickers hardness values for each material. Red are PECs, Grey are PPC, and blue is PVC.

# Literature Review

## Retention

Retention is the phase of orthodontic treatment that attempts to keep teeth in the corrected position after the removal of appliances and completion of treatment<sup>1</sup>. Without proper retention, orthodontic relapse will occur and tooth position or arch relationship will have a tendency to return to their initial presentations prior to treatment<sup>1,2</sup>. Four factors have been implicated in causing orthodontic relapse: forces from periodontal and gingival tissues, forces from orofacial soft tissues, occlusal forces, and post treatment growth and development<sup>3</sup>. If the teeth are in an unstable position at the completion of orthodontic treatment, forces from orofacial soft tissues or occlusal forces will cause relapse<sup>4</sup>. Gingival fibers require time to reorganize and remodel taking from 4-6 months for the reorganization of the gingival collagen fibers and up to 232 days for elastic supracrestal fibers; until this remodeling occurs elastic recoil of the teeth toward their original position occurs<sup>3,4</sup>. Unfavorable growth patterns, which originally lead to the development of the malocclusion, will continue through adult years and may contribute to a deterioration of occlusal relationships<sup>4,5</sup>. Even with completion of growth, relapse in the form of crowding has been shown to occur up to 20 years post-retention<sup>5</sup>.

The goal of the retention phase of orthodontics is to keep teeth in their corrected positions following treatment. This can be accomplished with proper planning of the retention phase. Six factors have been discussed in planning the retention phase of treatment: obtaining informed consent, the original malocclusion and the patient's growth pattern, the type of

treatment performed, the need for adjunctive procedures to enhance stability, the type of retainer, and the duration of retention<sup>1,3</sup>. A suggested retention protocol with removable retainers is 3-4 months of full time wear excluding mealtimes, followed by nighttime wear for a minimum of 12 months or until completion of growth<sup>4</sup>.

## **Retainer History and VFR fabrication**

Beginning around 1914, retainers were traditionally fabricated from gold wire and vulcanite. After 1937, steel wire and acrylic became the norm with many variations of the design throughout the years<sup>6</sup>. Shanks in 1963 demonstrated both transparent retainers and a machine capable of producing them. The most common materials used were: cellulose acetate butyrate, polyurethane, polyvinylacetate-polyethylene polymer, polycarbonate-cycloac, and latex<sup>6</sup>. In 1971 Ponitz<sup>6</sup> described the technique for fabrication of clear thermoplastic vacuformed retainers (VFRs). A vacuum unit holds a plastic blank while a heating source with the optimal temperature range 370-390° F heat-softens the material. Once the thermoplastic material has reach the optimal plasticity, it is adapted over a plaster model of the patient's dentition by either negative or positive vacuum pressure, either pulling or pushing the thermoplastic onto a working study model. A knife edge disc on a mandrel is used to carve and shape the periphery of the VFR. The VFR is lifted off the model, and the edges are polished smooth.

Today, the most common thermoplastic materials used to fabricate VFRs are polyethylene copolymers and polypropylene polymers<sup>7</sup>. The differences between the two

polymers are that acrylic can be bonded to polyethylene copolymer and it is more esthetic due to transparency of the material, whereas polypropylene is more durable and flexible<sup>7</sup>.

The retainers used in the modern orthodontic practice have not progressed since the steel wire and acrylic retainers of 1937 and the VFR of Ponitz in 1971. However, several retainer designs using these basic building materials have evolved over time. These designs have lacked any scientific evidence for use and are based on personal preference and other criteria<sup>1</sup>. In 2010, Valiathan and Hughes<sup>8</sup> conducted a survey of active members of the American Association of Orthodontists to assess the frequency of usage and prescribed wear time of various types of retainers following comprehensive treatment. The most commonly used retainers in the maxillary arch were Hawley retainers (58.2%), followed by VFRs (30.4%), fixed palatal retainers (2.4%), and spring aligners (1.1%)<sup>8</sup>. In the mandibular arch, fixed lingual retainers (40.2%) were used more frequently, followed by Hawley retainers (28.1%), VFRs (18.2%), and spring aligners (8.9%)<sup>8</sup>. Wear time was prescribed at 9 months full-time for removable retainers followed by indefinite part-time wear; 75.9% of orthodontists did not instruct patients to remove fixed retainers. Patients prescribed Hawley retainers were recommended longer fulltime wear than VFR<sup>8</sup>.

## **Attributes of VFRs**

Benefits of using VFR's include: ease of fabrication (including minimal time, skill and materials for construction) ease of delivery, and low cost<sup>9-11</sup>. The absence of any technical proficiency in wire bending allows delegation of the fabrication of VFR to auxiliary personnel in the orthodontic office<sup>12</sup>. VFRs are also durable, easily cleansable, small in size and esthetic<sup>13</sup>.

VFR survival times have been found in one study to be comparable with traditional Hawley retainers<sup>14</sup>. VFRs have been shown to hold corrections of lower anterior teeth more effectively than Hawley retainers and are more cost-effective<sup>15</sup>. The majority of patients also prefer VFRs to Hawley retainers wearing them more, leading to a higher satisfaction rate with their treatment<sup>16,17</sup>. Aside from retention, VFRs can also be used to produce minor tooth movements<sup>6,7</sup> or as bleaching trays<sup>18</sup>.

The major drawbacks of VFRs are their tendency to open the bite and their low durability<sup>10</sup>. VFRs have also been shown to inhibit relative vertical tooth eruption, or “settling” of the occlusion<sup>19</sup>. Low durability can result in broken VFRs, requiring additional financial cost to replace them, and an increase in the risk of orthodontic relapse if the broken retainer is not replaced in a timely fashion. Conversations with orthodontists also indicate that retainer fracture<sup>20</sup> and staining are problematic in orthodontic practice; however, there have been no reports of fracture frequency or noncompliance as a result of staining or wear.

## **Previous Research on VFR Materials**

As thermoplastic polymers are highly viscoelastic materials the environment and forming procedures have marked effects on their mechanical properties<sup>21</sup>. The elastic moduli and tensile yield stress of thermoplastic materials used for fabrication of invisible retainers are affected by the thermoforming process as well as immersion in water at 37 degrees for 24 hours<sup>21</sup>. The elastic moduli of amorphous thermoplastics were shown to increase after thermoforming and immersion in water at 37 degrees for 24 hours. The elastic moduli of semi-crystalline thermoplastics were generally shown to decrease after thermoforming and



immersion in water at 37 degrees for 24 hours. The tensile yield stress decreased for all the thermoplastic materials tested. The thermoplastics have also been shown to absorb water to different degrees over a 2 week period<sup>21</sup>.

The effect of oral cleansing agents on the essential work of fracture (EWF) and plastic work of fracture (PWF) for two thermoplastic materials has been investigated<sup>20</sup>. Polyethylene copolymer (Tru-Tain Splint) and polypropylene polymer (Essix C+) sheets were stored in a cleansing agent for 160 hours at 25 degrees and then tested. The polypropylene polymer showed higher EWF after storage in hydrogen peroxide versus storage in distilled water<sup>20</sup>. The polypropylene polymer showed higher EWF after storage in Crest Pro Health mouth rinse versus the polyethylene copolymer<sup>20</sup>. The polypropylene polymer exhibited lower PWF after storage in hydrogen peroxide than with any other storage conditions<sup>20</sup>. The polypropylene polymer exhibited higher PWF than the polyethylene copolymer after being stored dry, and in distilled water and Original Listerine<sup>20</sup>. The authors concluded that all tested cleansers could be used to clean thermoplastic orthodontic retainers without increasing the risk of fracture<sup>20</sup>.

## **Wear testing**

Wear is an important property used to assess the longevity of dental materials. There has been no in vitro device capable of accurately simulating and predicting clinical wear and studies have established only modest correlations between in vivo and in vitro wear of natural teeth and dental materials<sup>12,22,23</sup>. If wear testing of a contact free occlusal area is desired, a three body wear test composed of an antagonist abrader that only contacts the material of interest through an interposed suspension of an abrasive medium is used<sup>24</sup>. However, if one is

simulating wear of an occlusal contact area, then often a two body wear test is utilized composed of the antagonist abrader directly contacting the material to be tested; usually pin on disc tests or chewing simulators are used<sup>25-28</sup>.

Choosing a standardized material for the antagonist abrader has sparked discussion and disagreement amongst many researchers. One would consider enamel to be the ideal abrader, however there are many difficulties associated with using this material. Standardization of enamel abrader shape is difficult to accomplish<sup>29</sup>. The hardness of superficial and deep enamel as well as superficial and deep dentin are significantly different and therefore could produce variability in results<sup>29</sup>, and natural human cusps are difficult to harvest in large quantities<sup>30</sup>. Steatite ceramic spheres have been advocated as ideal antagonist abraders due to their ease of standardization, hardness that is similar to enamel, and well correlated wear rates and coefficients of friction in comparison to enamel<sup>31</sup>. Other researchers have opposed the use of steatite claiming this material has twice the hardness of enamel<sup>30,32</sup>. These authors have suggested the use of IPS classic ceramic, claiming that it has similar wear and other tribological characteristics to enamel<sup>30,32</sup>.

The extent of wear produced in in vitro tests can be quantitated using a variety of methods including gravimetric analysis and mechanical surface profiling with a sharp stylus. More recently, laser profilometry has become popular for assessing wear of many different types of materials in many industries. The technique utilizes infra-red light emitted from a semiconductor laser in the sensor onto the object surface. The light is then reflected back from the object and split into two beams that are focused on a set of photodiodes. A movable lens, suspended in the sensor is continuously adjusted to ensure the focal spot of the beam is

always coincident with the object surface. As the laser encounters variability in the surface of the object being measured, the beam displaces from the photodiodes causing the movable lens in the sensor to move and compensate. This movement in the lens is measured and provides the surface displacement of the object (object topography)<sup>33</sup>. Laser profilometry offers the advantage of being non-destructive, but may have the short coming of being unable to measure extremely rough surfaces with steep wear facets<sup>33</sup>.

## Previous Research on VFR Wear

The wear resistance of VFR thermoplastics has been investigated in two previous studies. Both studies<sup>7,12</sup> used steatite abraders and measured wear depth to assess wear resistance. Gardner et al.<sup>12</sup> created wear on three different thermoplastics: Essix C+ (PPC), Invisacryl C (PPC) and TR sheet material (PEC). Gardner formed the thermoplastics on a stone model using a positive pressure machine and mounted them to a wear machine, which was run at 25 kg (~245 N) for 1000 cycles in a 37 °C bath to simulate a two body wear test. The antagonist used was steatite sphere abrader with a diameter of 9.5 mm, which was run in a linear path for approximately 1 cm. The steatite abrader was replaced after each test. Wear changes were assessed with surface laser profilometry and showed that the polyethylene copolymer thermoplastic exhibited greater resistance to wear than the two polypropylene based thermoplastics.

Raja et al.<sup>7</sup> studied four different thermoplastics: Essix C+ (PPC), Essix Ace (PEC), Duran (PEC), and Tru-Tain (PEC). The materials were formed prior to wear testing on an acrylic block in a positive pressure machine and were run in the wear testing machine with 460 g (~4.5 N) of

force at 1000 cycles. Steatite spheres with a diameter of 8 mm were used as the abrader and replaced for each new test. One cycle is represented by the steatite spheres moving in a linear horizontal path of 16 mm to the right and then 16mm back to the left. Wear changes were assessed with surface profilometry and found that the three polyethylene co-polymers exhibited greater resistance to wear than the polypropylene based thermoplastic. Raja et al.<sup>7</sup> also found that Essix Ace had greater wear resistance than Tru-Tain. These two previous wear resistance studies show similar results indicating that under in vitro conditions polyethylene co-polymers have superior wear resistance to polypropylene based thermoplastics<sup>7,12</sup>.

## References:

1. Littlewood SJ, Millett DT, Doubleday B, Bearn DR, Worthington HV. **Retention procedures for stabilising tooth position after treatment with orthodontic braces.** *Cochrane Database Syst Rev.* 2004;(1)(1):CD002283
2. Littlewood SJ, Mitchell L. *Retention. An introduction to orthodontics.* 4th ed. Oxford University Press; 2013.
3. Melrose C, Millett DT. **Toward a perspective on orthodontic retention?** *American Journal of Orthodontics and Dentofacial Orthopedics.* 1998;113(5):507K514.
4. Proffit WR, Fields HW, and Sarver DM. *Contemporary Orthodontics.* 5th ed. St. Louis: Mosby, 2013.
5. Little RM, Riedel RA, Artun J. **An evaluation of changes in mandibular anterior alignment from 10 to 20 years post-retention.** *American Journal of Orthodontics and Dentofacial Orthopedics.* 1988;93(5):423K428.
6. Ponitz RJ. **Invisible retainers.** *American Journal of Orthodontics and Dentofacial Orthopedics.* 1971;59(3):266K272.
7. Raja TA, Littlewood SJ, Munyombwe T, Bubb NL. **Wear resistance of four types of vacuum formed retainer materials: A laboratory study.** *Angle Orthod.* 2014; 84(4):656K664.

8. Valiathan M, Hughes E. **Results of a survey based study to identify common retention practices in the United States.** *American Journal of Orthodontics and Dentofacial Orthopedics.* 2010;137(2):170K7; discussion 177.
9. McNamara JA, Kramer KL, Juenker JP. **Invisible retainers.** *J Clin Orthod.* 1985;19(8):570K578.
10. Wang F. **A new thermoplastic retainer.** *J Clin Orthod.* 1997;31(11):754K757.
11. Sheridan JJ, LeDoux W, McMinn R. **Essix retainers: Fabrication and supervision for permanent retention.** *J Clin Orthod.* 1993;27(1):37K45.
12. Gardner GD, Dunn WJ, Taloumis L. **Wear comparison of thermoplastic materials used for orthodontic retainers.** *American Journal of Orthodontics and Dentofacial Orthopedics.* 2003;124(3):294K297.
13. Mai W, He J, Jiang Y, Huang C, Li M, Yuan K, Kang N, **Comparison of vacuum-formed and Hawley retainers: a systematic review,** *American Journal of Orthodontics and Dentofacial Orthopedics;* 145 (6), pp. 720-727
14. Sun J, Yu YC, Liu MY, Chen L, Li HW, Zhang L, Zhou Y, Ao D, Tao R, Lai WL, **Survival Time Comparison between Hawley and Clear Overlay Retainers: A Randomized Trial,** *J Dent Res*
15. Rowland H, Hichens L, Williams A, et al. **The effectiveness of Hawley and vacuum formed retainers: A single center randomized controlled trial.** *American Journal of Orthodontics and Dentofacial Orthopedics.* 2007;132(6):730K737.

16. Hichens L, Rowland H, Williams A, et al. **Cost-effectiveness and patient satisfaction: Hawley and vacuum-formed retainers.** *The European Journal of Orthodontics*. 2007;29(4):372K378.
17. Mollov ND, Lindauer SJ, Best AM, Shroff B, Tufekci E, **Patient attitudes toward retention and perceptions of treatment success.**, *Angle Orthod*. 2010 Jul;80(4):468-73. doi: 10.2319/102109-594.1.
18. Sheridan JJ, Armbruster P. **Bleaching teeth during supervised retention.** *J Clin Orthod*. 1999;33(6):339K344.
19. Sauget E, Covell DA, Boero RP, Lieber WS. **Comparison of occlusal contacts with use of hawley and clear overlay retainers.** *Angle Orthod*. 1997;67(3):223K230.
20. Pascual AL, Beeman CS, Hicks EP, Bush HM, Mitchell RJ. **The essential work of fracture of thermoplastic orthodontic retainer materials.** *Angle Orthod*. 2010;80(3):554K561.
21. Ryokawa H, Miyazaki Y, Fujishima A, Miyazaki T, Maki K. **The mechanical properties of dental thermoplastic materials in a simulated intraoral environment.** *Orthodontic Waves*. 2006;65(2):64K72.
22. Powers JM, Ryan MD, Hosking DJ, Goldberg AJ, **Comparison of in vitro and in vivo wear of composites** *J Dent Res*, 62 (1883), pp. 1089–1091

23. Lutz F, Phillips RW, Roulet JF, Setcos JC, **In vivo and in vitro wear of potential posterior composites** J Dent Res, 63 (1984), pp. 914–920
24. Lambrechts P (1983) **Basic properties of dental composites and their impact on clinical performance** (thesis). Leuven, Belgium: Catholic University of Leuven
25. Krejci I, Lutz F, Zedler C (1992). **Effect of contact area size on enamel and composite wear.** J Dent Res 71:1413-1416.
26. Rice SL, Bailey WF, Pacelli PF 3rd, Blanck WR (1982). **Influence of enamel stylus stiffness on the sliding wear behavior of a composite restorative.** J Dent Res 61:493-496.
27. DeLong R, Douglas WH (1983). **Development of an artificial oral environment for the testing of dental restoratives: bi-axial force and movement control.** J Dent Res 62:32-36.
28. Roulet JF (1987). **Degradation of dental polymers.** Basel: Karger. Schroeder HE (1992). **Orale Strukturbiologie.** 4th rev. ed. Stuttgart: Thieme.
29. Zheng J; Zhou ZR; Zhang J; Li H; Yu Y; **On the friction and wear behavior of human tooth enamel and dentin.** Wear 2003; 255:967-974)
30. Krejci I, Albert P, and Lutz P; **The Influence of Antagonist Standardization on Wear.** JDR February 1999 vol. 78 no. 2 713-719)



31. Wassel RW, McCabe JF, Walls AWK, **Wear characteristics in a two-body wear test** *Dental Materials*, 10 (1994), pp. 269–274

32. Shortall AC, Hu XQ, Marquis PM. **Potential counter sample materials for in-vitro simulation wear testing.** *Dent Mater.* 2002;18:246–254

33. **UBM website**

data[https://www.researchgate.net/publication/229373349\\_UBM\\_Laser\\_Profilometry\\_and\\_Lithic\\_Use-Wear\\_Analysis\\_A\\_Variable\\_Length\\_Scale\\_Investigation\\_of\\_Surface\\_Topography](https://www.researchgate.net/publication/229373349_UBM_Laser_Profilometry_and_Lithic_Use-Wear_Analysis_A_Variable_Length_Scale_Investigation_of_Surface_Topography)

## **Appendix A: Recommendations and Future Research:**

There are several limitations to this study. First, it is an in vitro rather than in vivo study, as an in vivo would be much more complex and expensive to conduct, and difficult to standardize and reproduce. As stated previously, there is no in vitro device capable of accurately simulating in vivo wear. Each in vitro wear simulator differs in mechanism and results of wear simulation. It would be beneficial to analyze the samples under similar experimental protocols as the previous authors to determine if this was the determinant of the variation in results. Second, imaging of the wear facets proved to be difficult with the inability to provide three dimensional volumetric data, which ultimately would have produced more accurate results (i.e. less drop out of data due to poor surface reflections). Initially the experimental protocol was to prescan each sample prior to wear then again after wear, however the profilometer was unable to capture the data completely and a direct comparison of pre and post wear surface could not be obtained. Surface imaging might have been improved by an initial coating of the surface of the wear trace to enhance the return laser signal. A suggestion for further research would include proper three dimensional imaging and a volumetric analysis of the various groups. The use of a stylus profilometer with narrow cross sections could provide an accurate volumetric loss. However, this device does make physical contact against the specimen and may alter its surface. Future research could include an analysis of the effect of saliva uptake of the samples in relation to wear resistance by analyzing the thermoplastics after soaking then in a saliva medium for various time points.

## Appendix B: Reported Values and Statistical Analysis

sample	Maximum depth loss um					
	ACE	ULTRA	ENDURE	C+	INVIS C	PLUS
1	164.766	148.264	352.9400	139.636	115.046	107.616
2	211.975	219.171	257.9250	114.051	134.006	230.037
3	159.146	186.202	275.1430	122.159	142.446	145.122
4	229.63	165.358	334.1230	110.888	166.721	197.652
5	170.15	204.103	304.9400	179.679	176.275	211.687
6	139.492	201.731	386.7760	110.055	182.188	114.259
7	116.941	223.907	337.3980	192.984	153.807	173.83
8	152.34	196.58	297.0330	87.8361	116.293	126.758
9	143.226	219.228	323.0420	74.8191	104.147	221.903
10	217.385	134.378	295.7020	131.911	151.916	102.714
11	99.3236	225.08	295.9670	148.436	99.9427	209.53
12	151.765	160.182	297.7880	85.6999	141.721	130.17

Mean	163.0116333	190.3487	313.2314	124.8462	140.3757	164.2732
SD	39.5710432	31.34896	35.40263	36.20244	27.40316	48.2286
SEM	11.42317622	9.049665	10.21986	10.45074	7.910612	13.9224
N	12	12	12	12	12	12

Sample	net weight loss (g)					
	ACE	ULTRA	ENDURE	C+	INVIS C	PLUS
1	0.0047	0.0046	0.0052	0.0056	0.0052	0.0030
2	0.0042	0.0045	0.0052	0.0066	0.0041	0.0049
3	0.0039	0.0040	0.0068	0.0063	0.0038	0.0043
4	0.0052	0.0049	0.0049	0.0040	0.0048	0.0049
5	0.0068	0.0058	0.0092	0.0044	0.0053	0.0056
6	0.0035	0.0047	0.0062	0.0067	0.0051	0.0052
7	0.0051	0.0039	0.0071	0.0047	0.0042	0.0041
8	0.0068	0.0043	0.0070	0.0043	0.0034	0.0063
9	0.0048	0.0049	0.0062	0.0036	0.0055	0.0068
10	0.0074	0.0060	0.0064	0.0044	0.0057	0.0072
11	0.0051	0.0094	0.0068	0.0047	0.0070	0.0088
12	0.0053	0.0047	0.0086	0.0041	0.0052	0.0062

Mean	0.0052	0.0051	0.0066	0.0050	0.0049	0.0056
SD	0.0012	0.0015	0.0013	0.0011	0.0010	0.0016
SEM	0.0003	0.0004	0.0004	0.0003	0.0003	0.0005
N	12	12	12	12	12	12

sample	hardness					
	ACE	ULTRA	ENDURE	C+	INVIS C	PLUS
Value on impressor	63.5	64	69	45	55	67
	63	64	70	44	56	66.5
	64	64	72	45	54	67
average	63.5	64.0	70.3	44.7	55.0	66.8
Vickers preforming	54	55	69	29	42	60
Vickers after forming	48.5	57.5	70	25	37.5	58

material	density	density	ave	wt loss( g)	Volume loss (cm3)
	1	2			
Invis C	0.9912	0.9886	0.9899	0.004942	0.004992
C+	0.9872	0.9914	0.9893	0.00495	0.005004
ULTRA	1.1644	1.1739	1.16915	0.005142	0.004398
ACE	1.23	1.229	1.2295	0.005233	0.004256
PLUS	1.1767	1.1775	1.1771	0.005608	0.004764
Endure	1.3013	1.3022	1.30175	0.006633	0.005095

Sample	Volume Loss					
	ACE	ULTRA	ENDURE	C+	INVIS C	PLUS
1	0.0038	0.0039	0.0040	0.0057	0.0053	0.0025
2	0.0034	0.0038	0.0040	0.0067	0.0041	0.0042
3	0.0032	0.0034	0.0052	0.0064	0.0038	0.0037
4	0.0042	0.0042	0.0038	0.0040	0.0048	0.0042
5	0.0055	0.0050	0.0071	0.0044	0.0054	0.0048
6	0.0028	0.0040	0.0048	0.0068	0.0052	0.0044
7	0.0041	0.0033	0.0055	0.0048	0.0042	0.0035
8	0.0055	0.0037	0.0054	0.0043	0.0034	0.0054
9	0.0039	0.0042	0.0048	0.0036	0.0056	0.0058
10	0.0060	0.0051	0.0049	0.0044	0.0058	0.0061
11	0.0041	0.0080	0.0052	0.0048	0.0071	0.0075
12	0.0043	0.0040	0.0066	0.0041	0.0053	0.0053
Mean	0.0043	0.0044	0.0051	0.0050	0.0050	0.0048
SD	0.0010	0.0013	0.0010	0.0011	0.0010	0.0013
SEM	0.0003	0.0004	0.0003	0.0003	0.0003	0.0004

## Appendix C: Images of Sample Fabrication

